Fort Ord Site UXO Classification Demonstration Using Fully Polarimetric GPR ESTCP Project 199902

Chi-Chih Chen
The Ohio State University ElectroScience Laboratory
1320 Kinnear Rd
Columbus, OH 43212

Kevin O'Neill
US Army Corps of Engineers
Engineer Research and Development Center (ERDC)
Cold Regions Research and Engineering Laboratory (CRREL)
72 Lyme Road
Hanover, NH 03755

August 2005

Report Documentation Page

Form Approved
OMB No. 0704-0188

<table>
<tr><td colspan="2">1. REPORT DATE
AUG 2005</td><td colspan="2">2. REPORT TYPE</td><td colspan="2">3. DATES COVERED
00-00-2005 to 00-00-2005</td></tr>
<tr><td colspan="4" rowspan="3">4. TITLE AND SUBTITLE
Fort Ord Site UXO Classification Demonstration Using Fully Polarimetric GPR</td><td colspan="2">5a. CONTRACT NUMBER</td></tr>
<tr><td colspan="2">5b. GRANT NUMBER</td></tr>
<tr><td colspan="2">5c. PROGRAM ELEMENT NUMBER</td></tr>
<tr><td colspan="4" rowspan="3">6. AUTHOR(S)</td><td colspan="2">5d. PROJECT NUMBER</td></tr>
<tr><td colspan="2">5e. TASK NUMBER</td></tr>
<tr><td colspan="2">5f. WORK UNIT NUMBER</td></tr>
<tr><td colspan="4">7. PERFORMING ORGANIZATION NAME(S) AND ADDRESS(ES)
Ohio State University,Electroscience Laboratory,1320 Kinnear Rd,Columbus,OH,43212</td><td colspan="2">8. PERFORMING ORGANIZATION REPORT NUMBER</td></tr>
<tr><td colspan="4" rowspan="2">9. SPONSORING/MONITORING AGENCY NAME(S) AND ADDRESS(ES)</td><td colspan="2">10. SPONSOR/MONITOR’S ACRONYM(S)</td></tr>
<tr><td colspan="2">11. SPONSOR/MONITOR’S REPORT NUMBER(S)</td></tr>
<tr><td colspan="6">12. DISTRIBUTION/AVAILABILITY STATEMENT
Approved for public release; distribution unlimited</td></tr>
<tr><td colspan="6">13. SUPPLEMENTARY NOTES</td></tr>
<tr><td colspan="6">14. ABSTRACT</td></tr>
<tr><td colspan="6">15. SUBJECT TERMS</td></tr>
<tr><td colspan="3">16. SECURITY CLASSIFICATION OF:</td><td rowspan="2">17. LIMITATION OF ABSTRACT
Same as Report (SAR)</td><td rowspan="2">18. NUMBER OF PAGES
51</td><td rowspan="2">19a. NAME OF RESPONSIBLE PERSON</td></tr>
<tr><td>a. REPORT
unclassified</td><td>b. ABSTRACT
unclassified</td><td>c. THIS PAGE
unclassified</td></tr>
</table>

Table of Contents

List of Figures

List of Tables

`

Chapter 1 Introduction

The OSU/ESL broadband, full-polarimetric ground penetrating radar (GPR) has been applied for UXO classification under the support of ESTCP project beginning in 1999. Since then the system has been used to collect radar data and perform blind UXO classification at several UXO sites including Tyndall AFB, FL ("Tyndall"), Blossom Point, MD (BP) and Jefferson Proving Ground, IN (JPG). The results of these field tests have been documented in previous ESTCP reports. The fourth and final field demonstration was conducted at the former Fort Ord, CA, from October 29 to November 3 of 2001. The first blind classification results were then reported to ESTCP prior to the reception of the true depth information. This report presents documentation of the test and the results of classification processing, with and without that depth information.

The objective of the Fort Ord test is to evaluate classification performance in a sandy environment, given the improvements in survey and processing systems developed since the Tyndall demo. Detailed site information for the Fort Ord UXO site can be found in the “Ordnance Detection and Discrimination Study” (2000) prepared by the USA Environmental, Inc. Although the earlier Tyndall site was also a sandy site, that demo was performed more then three years ago with processing based only on single-position features. The improved classification algorithm utilizes late-time radar signatures including natural resonance [1][2] and detection of linear scattering polarization, as introduced during the Tyndall test [3]; and analysis of the spatial variation of data features as introduced during the BP demo [4][5]. Multiple radar passes were also performed for each target spot. The final system combined multiple positions, multiple orientations, broad frequency range and fully polarimetric configuration. This provided additional time-position scattering features of early-time responses as well as the spatial distributions of the late-time UXO signatures. These improvements addressed the classification of UXO’s with large inclination angles and also shallow non-UXO objects.

Soil probe data showed that the sand in the Fort Ord site was quite dry throughout the measurement period in the whole area, with a relative permittivity of 3.5 and conductivity less than 0.004 S/m at 60 MHz. Electromagnetic wavelengths are shorter in soil than in the air. The low dielectric constant means that wavelengths were not shortened as much as they would have been in more moist soil. Since the maximum operational frequency is 800 MHz, this means that the minimum classifiable length is approximately 4 inches based on the range of resonant lengths for objects in this medium, i.e.

$$L \geq \frac{\lambda_d}{2} = \frac{c/\sqrt{\varepsilon_d}}{2f},$$

where $c = 3\times10^8$ m/s, $\varepsilon_d = 3.5$ and *f*= *800* MHz. Higher resonant frequencies associated with UXO shorter then 4 inches cannot be observed in these soil conditions with the current system, making the late-time classification algorithm inapplicable for correspondingly short objects. Because most targets of interest were longer than 4 inches, this should not pose much of a problem.

The general drift of our self-analyses in reports thus far is carried forth in the current report, namely: our system demonstrates definite discrimination capability, relative to random classification, and surveying success with our system is clutter limited. Moist soil diminishes target signal strength, and raises the effective clutter level due to reflections from surface and subsurface heterogeneities. Unfortunately, despite its dryness, the Ft Ord site was also strongly cluttered. In particular, it contained an astonishingly extensive network of tunnels with diameters ranging from 1 inch to 6 inches, evidently from snakes, small mammals, and especially badgers (the site is called "badger flats"). The openings of these tunnels were “everywhere”! One had to walk carefully to avoid stepping into these openings. Apparently, the badgers were quite active during the night, as many freshly dug openings were typically apparent on our morning arrivals at the site. From the radar point of view, this changing network of tunnels created a highly inhomogeneous medium that raised the clutter level. An empty tunnel that has a diameter less than the wavelength, as in this case, generated dominant scattered fields polarized in the direction transverse to the tunnel. If the tunnel is filled with water, the dominant scattered fields are polarized parallel to the tunnel orientation. Any animals present in the tunnels constituted strong scatterers, due to the high dielectric constant and conductivity of their bodies. A large badger could very well give stronger radar responses then a small UXO. The GPR data clearly indicate the extent of the problem. Figure 1 shows the cross-polarization GPR data collected at two known empty cells (#623 and #617). The horizontal axis corresponds to the antenna position and the vertical axis indicates the delay (i.e. arrival) time of the responses. This delay time is approximately proportional to the distance between the antenna and a subsurface feature causing some reflection. Each four nano seconds corresponds approximately to one foot distance. Note that this distance is not necessarily the depth since the response may come from directions other than the downward direction. The responses from these underground tunnels are clearly visible. Figure 2 provides an example (site #347) of the polarized nature of the tunnel responses by showing results from different polarizations and different scan directions. One sees that the same tunnel produces different scattering magnitude in different polarization channels and different scan

directions. The responses from these underground features set the clutter level of this site and thereby determine the effective sensitivity of the GPR radar.

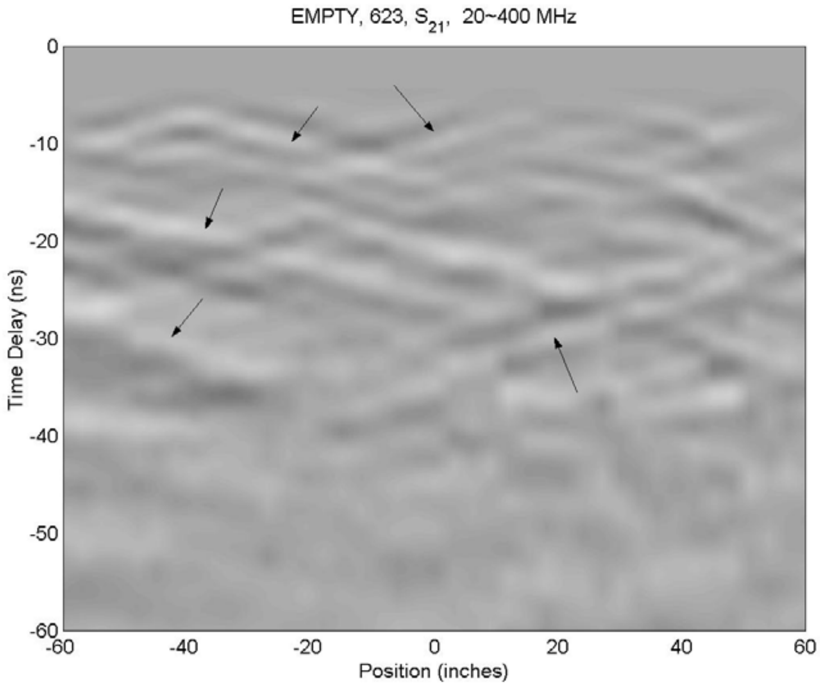

(a) Empty Site #623

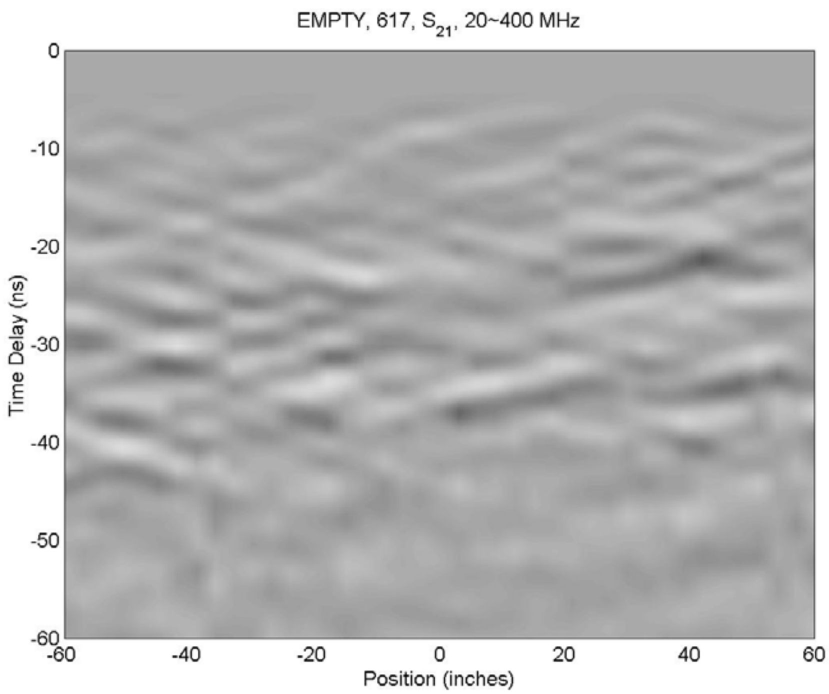

(b) Empty Site (#617)

Figure 1. GPR data (lower band 20~400 MHz) collected at known empty sites (a) #623 and (b) #617 indicate complicated underground tunnel networks.

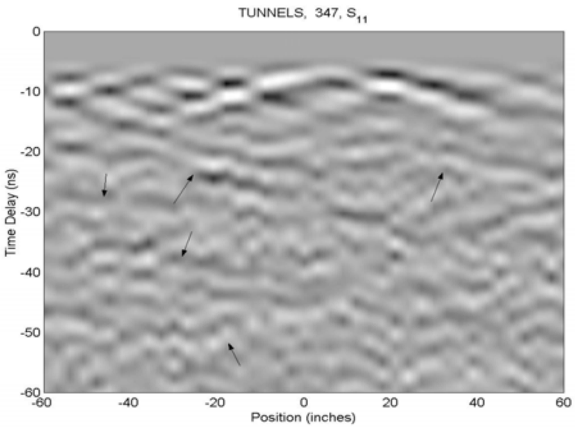

(a) S_{11}, Scan Angle = 116^{o}

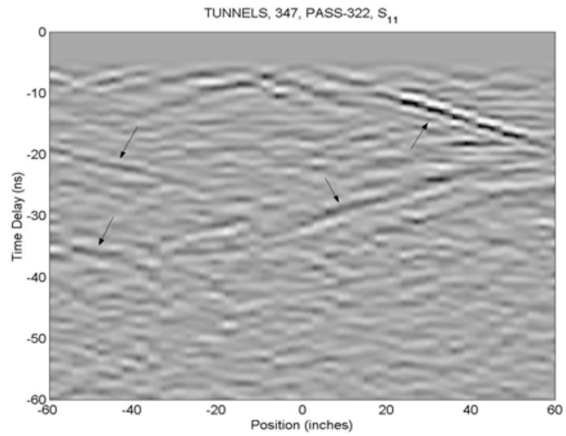

(d) S_{11}, Scan Angle = 322^{o}

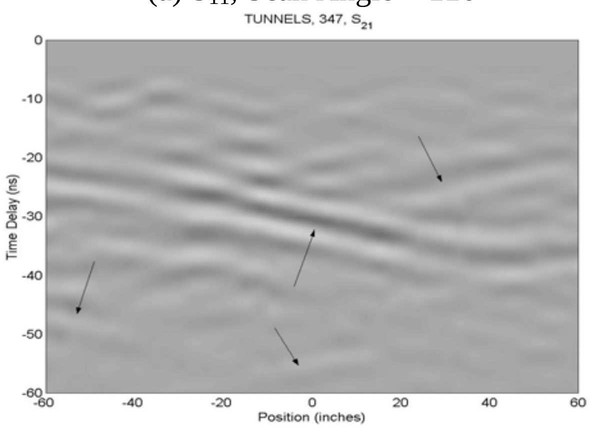

(b) S_{21}, Scan Angle = 116^{o}

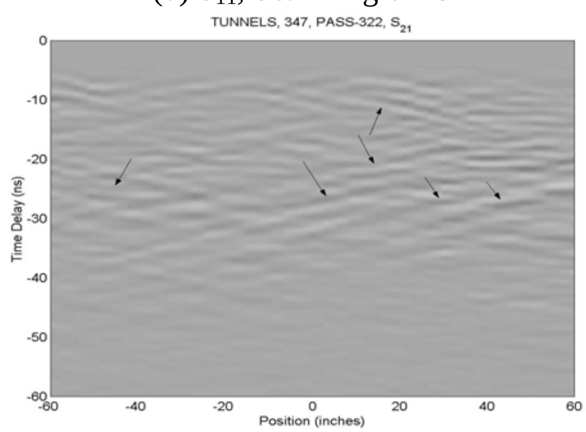

(e) S_{21}, Scan Angle = 322^{o}

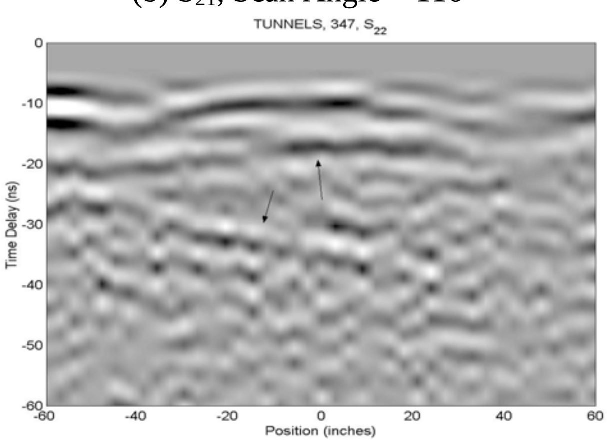

(c) S_{22}, Scan Angle = 116^{o}

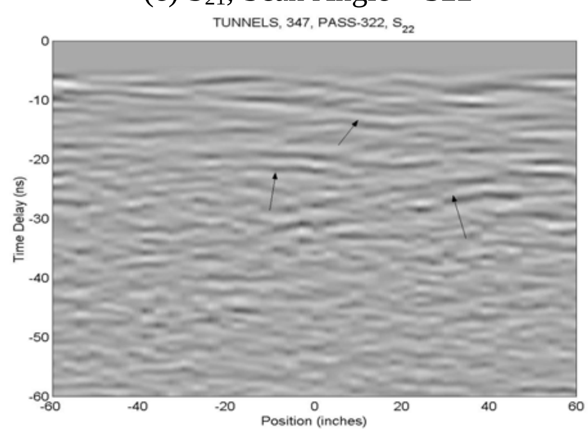

(f) S_{22}, Scan Angle = 322^{o}

Figure 2. Examples of tunnel responses observed in the GPR data (lower band 20~400 MHz) collected at Site #347 (fragment, 6-inch depth) for different polarizations and scan directions.

Chapter 2 Technology Description

2.1 System Description

The radar system consisted of a broadband fully-polarimetric horn-feb bowtie (HFB) antenna [1] developed by the OSU-ESL. It was towed behind a tractor, which also carried a laptop computer and a network analyzer HP8712 (Figure 3). The computer was for controlling the radar as well as signal processing. The commercial network analyzer was used as a step-frequency radar for collecting fully polarimetric data, including co-polarized (S_{11} and S_{22}) and cross-polarized (S_{21}) reflections. Stepped-frequency data from 10 MHz to 810 MHz at 2 MHz increments were collected along straight lines centered at each flagged “hot spot.” The flags were located by the site management team so as to simulate offsets from the target locations in the ground truth such as would occur in typical electromagnetic induction or magnetometer detection surveys. Each GPR survey line was 10 ft in length, with data taken at 3-inch increments. Positioning of the rig was based on markers on the front wheels. Both frequency domain and time domain data were displayed in near real time so that the operator could monitor the status of the operation. Although on-site processing could be performed immediately after each pass, the actual processing was performed overnight to maximize the data collection rate. The radar unit and the antenna were connected via a long 40-foot RF cable to provide a 120 ns delay, further isolating multiple reflections between the radar unit and the antenna’s input terminals.

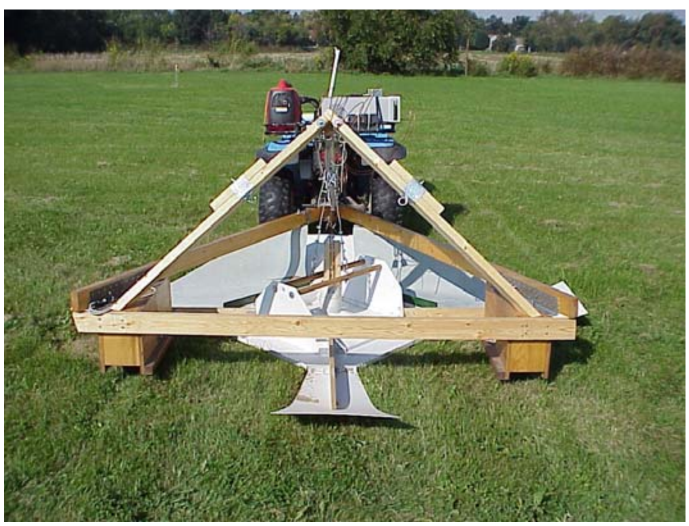

Figure 3. OSU/ESL UWB fully-polarimetric GPR system.

2.2 Measurement Approach

For each "hot spot," two straight line radar passes with orientations parallel and transverse to the azimuth orientation of a linear (elongated) object such as a UXO are needed for optimal classification. Since the orientation is not a known priori, this objective is approached iteratively.

First, a conventional metal detector was used to determine the unseen object's magnetic dipole orientation (if any). This was done by manually surveying near the flags using a hand-held vertical differential magnetometer (Schonstedt). An elongated object produces an axially oriented dipole, which is usually indicated by the presence of a null and sign change in the magnetometer data. A more accurate and efficient magnetometer than our handheld system would provide commensurately improved dipole determination. Our use of the Schonstedt was primarily for a "reality check" on flag position and clutter level, and for an elementary test of the virtues of combining the two technologies. If a magnetic dipole was observed, an initial radar pass was then oriented along this its orientation. If no magnetic dipole orientation was detected, an arbitrary direction was chosen for the initial pass.

The radar data collected from the 1st pass were processed to extract any late time linear polarization tendencies, which would indicate a dominant azimuthal target orientation. If the indicated GPR orientation was close to that of the apparent magnetic dipole in the 1st pass, the 2nd pass was oriented perpendicular to it. If the estimated orientation from the GPR data was significantly different from that provided by the metal detector, the 2nd and 3rd passes were oriented parallel and transverse to the estimated orientation, respectively. Notice that the 45^{o}-orientation pass adopted in the JPG test is not performed. Even though the S_{21} response can provide better detection, it turns out not to help the classification significantly without good S_{11} and S_{22} responses, which are usually stronger.

2.3 Feature Extraction

2.3.1 Feature Extraction Block Diagram

The procedure for extracting target features is shown Figure 4. Detailed algorithms for each block can be found in various publications [4][5][6]. The resultant features include Estimated Linear Factor (ELF), Estimated Target Orientation (ETO), Complex Natural Resonance (CNR), and depth (DEP). Many improvements have been reported in the previous report [5] and will not be repeated here. A new improvement for more accurate depth and length estimations is discussed below. This new algorithm was developed to deal with the JPG soil, where soil properties vary significantly with depth.

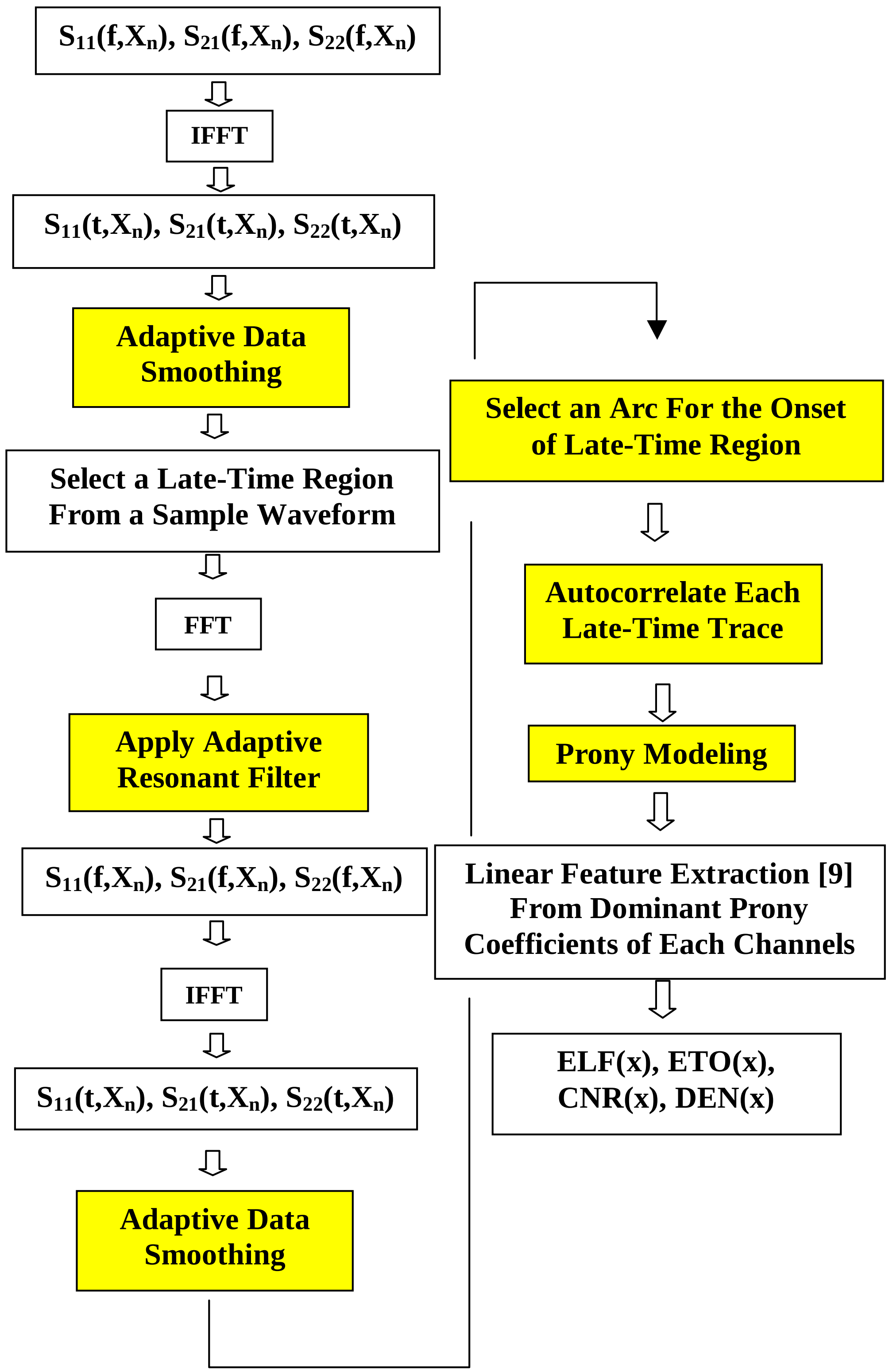

Figure 4. Block diagram of the OSU/ESL UXO feature extraction procedures.

2.4 UXO-Like/Non-UXO Discrimination Criteria

Figure 5 shows the flow chart for the new UXO classification criteria. This flow chart was established and improved based on responses of some canonical UXO and non-UXO objects encountered during the Tyndall and BP demos. The whole UXO classification procedure starts with inspection of the spatial distribution of the extracted ELF, that is, ELF plotted as a function of antenna position (the blue plots A,B,E,G, and H). Progress through the flow chart from this point is briefly described below. One can refer to [5] for more elaboration. In brief:

- If the ELF is low over most of the 10 foot scan region (scenario A), it indicates that the target does not have a linear shape and thus it is classified as a non-UXO object.

- If the ELF values near the target center are high (closer to one) as in scenario B, the object could be an UXO-like object, vertical plate or a vertically oriented curved metal such as horseshoe. The next thing to check is the scattering pattern, i.e. time-position plots, associated with a *transverse* pass, in which a horizontal UXO would have very weak response in the S_{11} channel. If strong responses are observed in the S_{11} channel at offset positions (C), it would not be a UXO. It could be large vertical plate, vertical horseshoe, vertical bent wire, etc. If the object shows good linear and resonance features in all passes but the ETO or resonant frequency seems to vary in different passes, it is probably a thin metal object with curved shapes.

- If there are two high-ELF regions next to the target center (double peaks, scenario E), it could be a vertical UXO or shallow clutter. The latter shows high ELF values when it is very close to one of the antenna arms. In either situation, the ETO will indicate an orientation aligned with the scan directions in all passes. Under scenario E, if the scattering pattern in the time-position plot shows strong responses in *both* S_{11} and S_{22} channels at the target center, it is likely a horizontal plate that has small L/D ratio. If the scattering pattern shows response only in the S_{11} channel and is weak over the target location, it could be a vertical UXO or small clutter depending on whether significant resonance is present.

- If a single peak region of high ELF values is offset to one side of target center (scenario G), it is probably an inclined UXO or a horizontal UXO with position offset. In this case, the ETO near the high ELF region should remain unchanged regardless of the scan direction.

- If ELF values vary drastically between 0 and 1 in a sort of random way (scenario H), its is either not a coherent target or the signal to clutter ratio (SCR) value is very poor.

The classification criteria discussed above were found to be very effective in discriminating UXO-like targets on the known target site. Each of these criteria may be developed into automatic classification procedures using pattern recognition, image correlation or neural network training techniques. However, at this moment, Figure 5 is implemented by training an operator using a training set and then having him or her make a classification decision by following the flow chart. This training is not difficult. Also, we show a comparison of results below that are consistent from one demo to the next, despite the subjectivity of the operators' judgments.

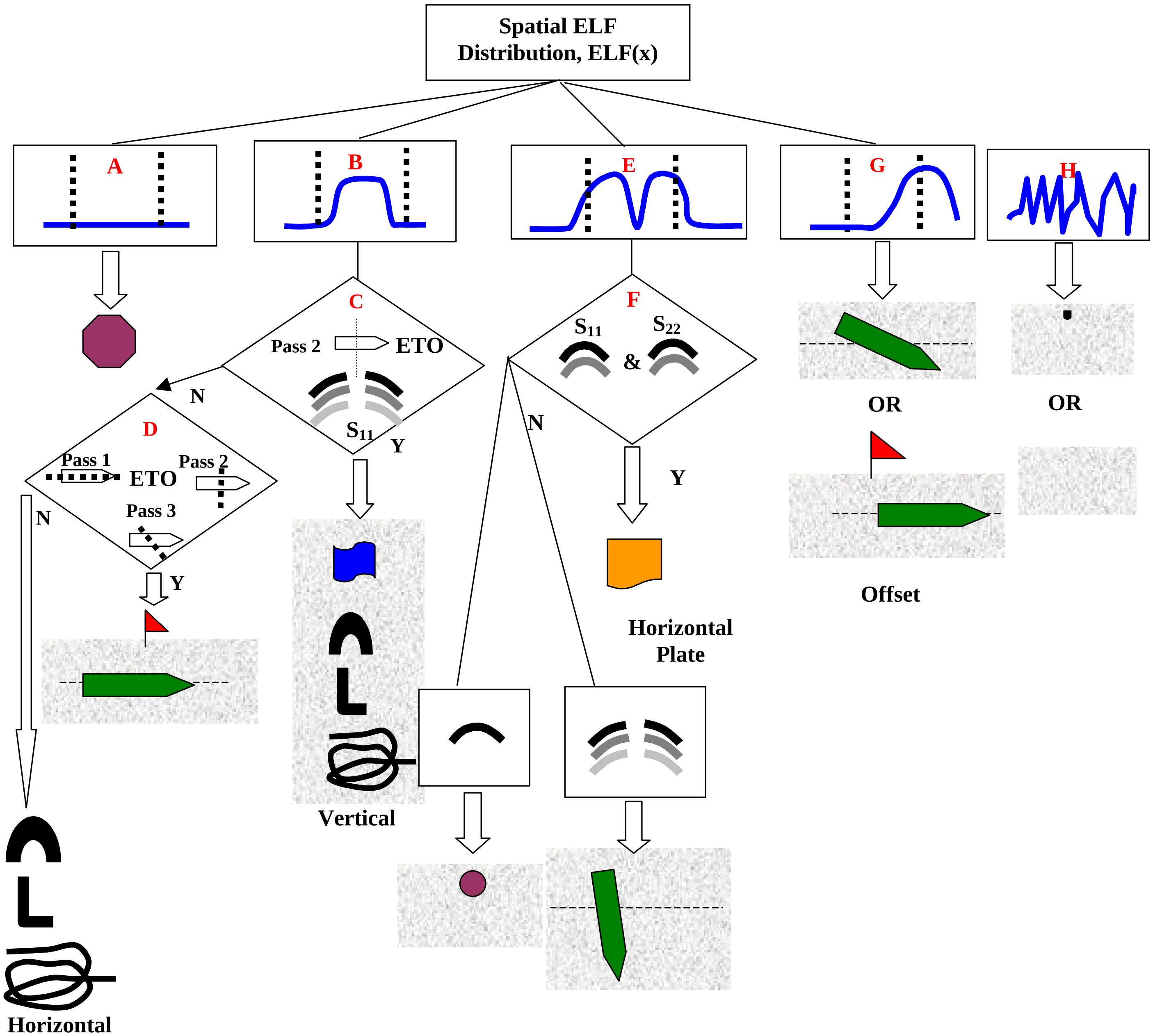

Figure 5. Improved UXO classification flow chart.

Chapter 3 UXO Classification Results

3.1 Blind Target Classification Results

The tables of blind classification results obtained with and without true-depth information are shown in Table 9 and Table 10 in Appendix A, using “TRUE UXO” and “UXO-LIKE” criteria, respectively. These tables serve as prioritized dig lists based on confidence levels derived from Round-1 results. The estimated features such as length, depth, and azimuthal orientation extracted from GPR data are included. Recall that “Round-1” results was obtained from a completely blind processing. “Round-2” results utilized the true-depth information to determine the correct onset of the late-time responses for targets that had larger discrepancy (>20cm) between the estimated depth from Round-1 and the true depth. “TRUE UXO” and “UXO-LIKE” are labels indicating what criteria determined whether an object in the ground truth list was considered to be a UXO. That is, TRUE UXO designates an object to be a UXO based on its actual identity, regardless of its geometry. On this basis, there are 63 UXO items, two empty sites and 32 clutter items. The clutter items include fragments, hot rocks, and debris (see Appendix B). The UXO items include three MKII grenades and two M9 rifle grenades. The UXO-LIKE criterion designates an object to be UXO if its length is greater than 4 inches (due to system frequency limitation) and its length-to-diameter (L/D) ratio is greater than three. Based on this criterion, there are 70 UXO-like items, two empty sites and 25 clutter items. Notice that, under this criterion, the clutter items include three MKII hand grenades (see Figure 6) that do not satisfy the L/D ratio criterion. Some clutter items were also designated as UXO-like objects under this criterion as indicated by the value of one in the “UXO-Like ID” column. Appendix B contains pictures of these clutter items. While use of the UXO-like criterion would mandate clearance of some non-UXO items, it is applied as one classification option in part for the sake of comparison to other survey systems. That is, it proceeds on the assumption that objects revealed to have such L/D ratios would appear on a dig list for virtually *any* survey system. In any case, it provides a good assessment of the GPR and processing performance *based on the data features under consideration*.

Figure 6. MKII Grenade

The causes for classification errors (missed UXOs and false alarms) will be examined shortly in the following section. A ROC curve is plotted based on variation of the processing "Confidence Level" as a threshold. Proceeding from high to low, these thresholds are

1. UXO = items classified as UXO with high confidence, all other items considered non-UXO
2. UXO = items classified as UXO with at least medium confidence, all other items = non-UXO
3. UXO = items classified as UXO with at least low confidence, all other items = non-UXO
4. UXO = items classified as clutter with low confidence plus all items classified as UXO (with any level of confidence), all other items considered non-UXO
5. UXO = items classified as clutter with at most medium confidence plus all items classified as UXO (with any level of confidence), all other items considered non-UXO

Table 1 through Table 4 display the UXO classification rate defined as <number of items classified as UXO (or UXO-like)/ total number of UXO (or UXO-like)> vs. false alarm rate, generated from the above threshold scheme. Theses results are also plotted in Figure 7. From these tables, it appears that the second round processing utilizing the true depth information does not appear to bring significant change in classification results. The current radar signatures only discriminate elongated objects - including rebars, cylinders or strips as well as UXO - from non-elongated objects such as chunks of metal or plates with similar side dimensions. Thus the classification system based on the UXO-like designation provides a better assessment of the effectiveness of the classification system at doing what it is designed for. In addition to the elongated shape (L/D ratio>2 or 3) limitation, the maximum operational frequency also limits the shortness of length of the target that can be classified correctly, as discussed in Chapter 1. From the results shown from Figure 7 to Figure 9, it is obvious that a more accurate classification is achieved for UXO-like objects.

It is quite interesting to observe that the classification performance for the current Fort Ord and the JPG V sites are very similar despite their radically different environments and target set. Somewhat different crews also operated at these two sites. This similarity of results is demonstrated in Figure 8 and Figure 9. The similarity also indicates the consistency of the classification algorithm shown in Figure 5, even though it was executed qualitatively by a trained person as opposed to an automatic algorithm. It is reasonable to expect a much better performance once more sophisticated training and pattern recognition algorithms are developed. Overall, the major performance limitation is that there are still significant numbers of UXO missed. Possible causes for the missing UXO's in the current demo will be examined in Section 3.1.2 below.

Table 1. UXO classification rate and false alarm rate based on confidence levels using "TRUE UXO" criteria (Round 1).

THRESHOLD	UXO AS CLUTTER	CLUTTER AS UXO	DETECTION RATE	FALSE ALARM RATE
UXO – "H"	26/63	8/34	0.413	0.235
UXO – "M"	31/63	10/34	0.492	0.294
UXO – "L"	37/63	16/34	0.587	0.470
CLUTTER – "L"	52/63	28/34	0.825	0.824
CLUTTER – "M"	58/63	30/34	0.920	0.882

Table 2. UXO classification rate and false alarm rate based on confidence levels using "TRUE UXO" criteria (Round 2).

THRESHOLD	UXO AS CLUTTER	CLUTTER AS UXO	DETECTION RATE	FALSE ALARM RATE
UXO – "H"	26/63	9/34	0.413	0.235
UXO – "M"	34/63	10/34	0.540	0.294
UXO – "L"	40/63	14/34	0.635	0.412
CLUTTER – "L"	55/63	28/34	0.873	0.824
CLUTTER – "M"	58/63	30/34	0.920	0.882

Table 3. UXO classification rate and false alarm rate based on confidence levels using "UXO-LIKE" criteria (Round 1).

THRESHOLD	UXO AS UXO	CLUTTER AS UXO	DETECTION RATE	FALSE ALARM RATE
UXO – "H"	32/70	2/27	0.457	0.074
UXO – "M"	37/70	4/27	0.529	0.148
UXO – "L"	44/70	9/27	0.629	0.333
CLUTTER – "L"	59/70	21/27	0.842	0.778
CLUTTER – "M"	64/70	24/27	0.914	0.889

Table 4. UXO classification rate and false alarm rate based on confidence levels using "UXO-LIKE" criteria (Round 2).

THRESHOLD	UXO AS UXO	CLUTTER AS UXO	DETECTION RATE	FALSE ALARM RATE
UXO – "H"	32/70	3/27	0.457	0.111
UXO – "M"	39/70	5/27	0.557	0.185
UXO – "L"	46/70	8/27	0.657	0.296
CLUTTER – "L"	61/70	22/27	0.871	0.815
CLUTTER – "M"	64/70	25/27	0.914	0.926

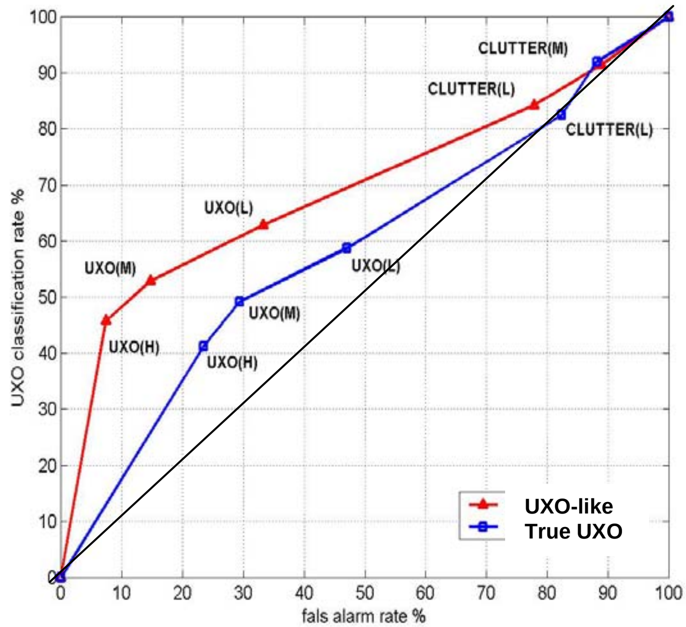

Figure 7. ROC curves for Ft Ord Demo, with blind UXO classification (Round-1), using confidence level as the thresholds, with 45° "line of no discrimination."

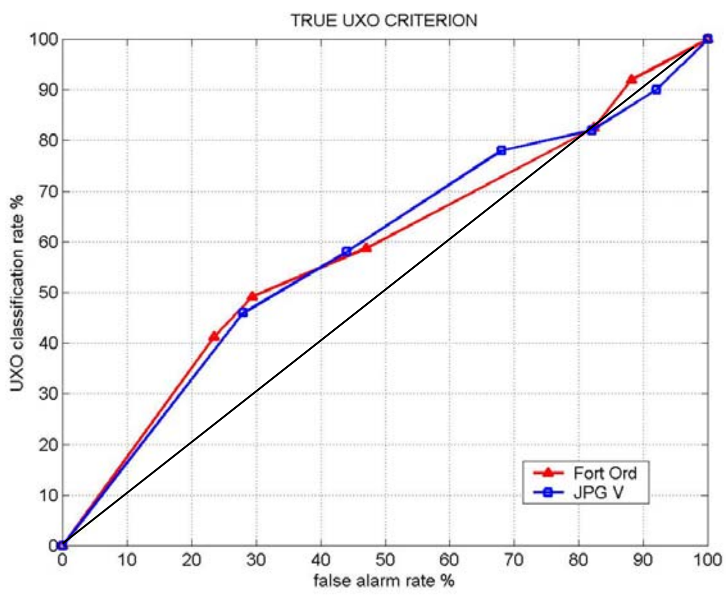

Figure 8. Comparison of ROC curves obtained from Fort Ord and JPG V sites, based on blind UXO classification (Round-1) using "TRUE UXO" criterion.

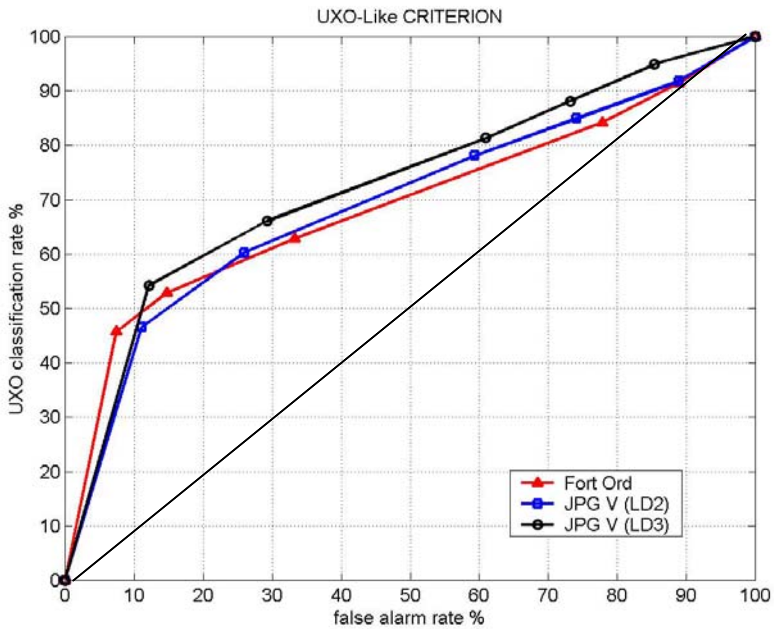

Figure 9. Comparison of ROC curves obtained from Fort Ord and JPG V sites based on blind UXO classification (Round-1) using "UXO-LIKE" criterion.

3.1.1 Feature Accuracy for Correctly Classified Items

The current UWB FP GPR system can estimate the length, depth, and azimuthal orientation of a buried UXO, based on the resonant frequency [1], delay time of target response, and eigenfunctions of the scattering matrix [3]. Since there are multiple passes for each target, these features are usually selected from the pass that gives best quality of features, i.e. minimal clutter. The extracted features of all targets measured at the Fort Ord site are included in the tables in Appendix A. Figure 10 summarizes the absolute length estimation error compared to the true length for correctly classified UXO-like items. Approximately 80% of the targets have a length error less than 5 inches. The cause for the 11" error in Item 490 is unknown. Figure 11 shows the azimuthal orientation error for correctly classified UXO-like items. The error is biased to approximately –40 degree, probably due to calibration error in the compass mounted on the GPR rig. The bias error notwithstanding, approximately 70% of the targets have an orientation error within 30 degrees of the true orientation. The absolute depth estimation error from Round-1 (i.e. blind) results is shown in Figure 12, indicating that the depths of most UXO-like items are overestimated by about 6 inches. Such an overestimation is most likely due to the selection of the impulse response (pulse onset or pulse peak) in the signal records. In our case, the peak of the first observable pulse was used. The time delay of this peak was determined relative to the time position of the response from a wire laid on the ground surface. Depth overestimation is likely for a UXO-like object that has a large inclination angle since stronger scattered fields may arise from body parts other than the shallowest point. Depths for items 545 and 497 are apparently incorrect, as opposed to merely inaccurate. This means that a response from some clutter in earlier time was picked for delay timing, due to its stronger magnitude compared to the later and weaker target response. In some cases, a small UXO at shallow depth may have been overlooked compared to deeper, stronger clutter, thus resulting in overestimated depth.

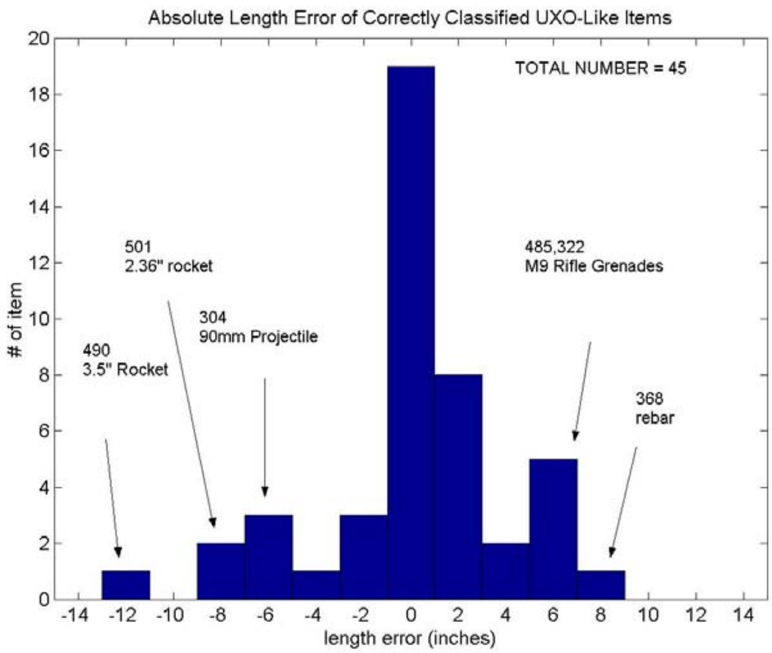

Figure 10. Absolute error of length estimation for correctly classified UXO-like items.

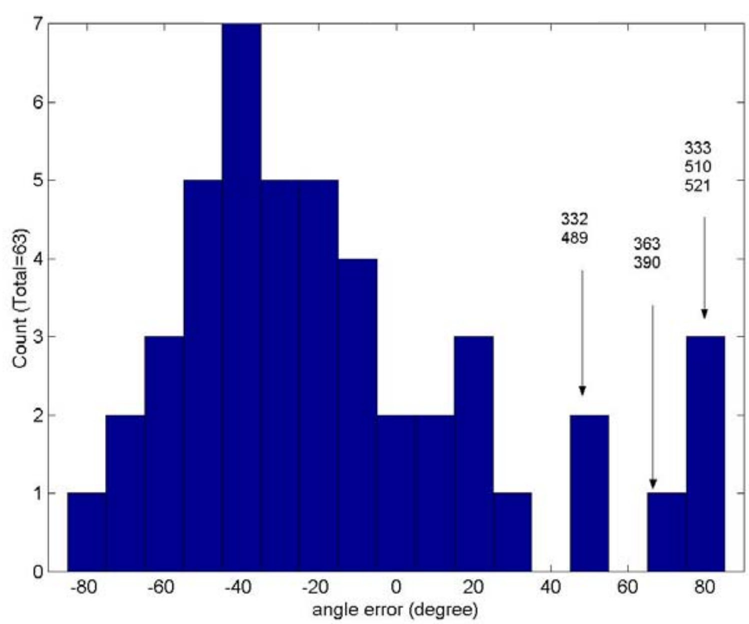

Figure 11. Absolute error of azimuth angle estimation for correctly classified UXO items.

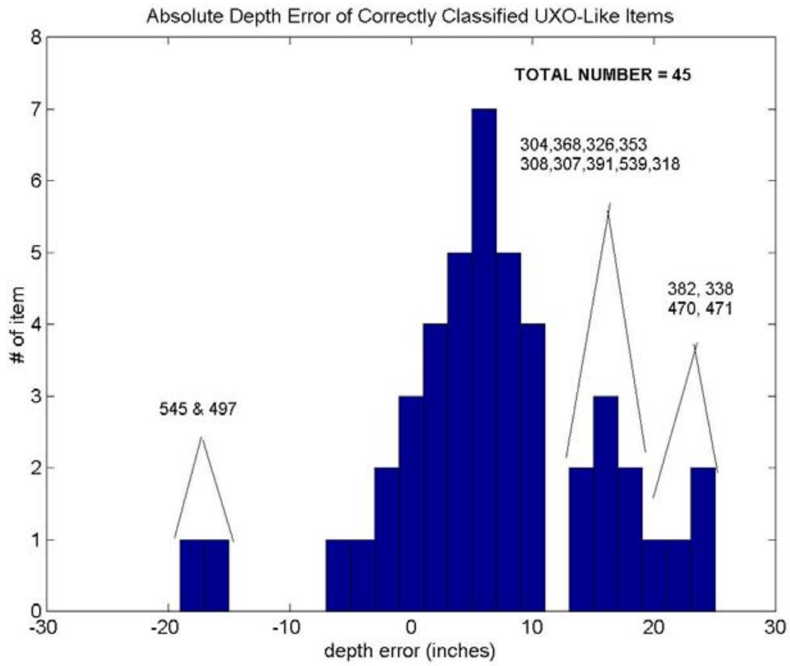

Figure 12 Absolute error of depth estimation for correctly classified items.

3.1.2 Causes of Missed UXO-Like Items

As mentioned earlier, the major concern of the current performance is that there are still significant numbers of UXO missed. Table 5 lists the UXO items that were missed during the Round-2 classification. First, note that 6 of the 18 near vertical UXO's were missed. Table 6 shows a list of near vertical UXO-like items with the missed ones highlighted in the 1st column. Most of the missed ones have a relatively greater depth compared to the others. Therefore, deep vertical UXO-like objects still present a challenging issue. Also, while not classified as UXO by the processing Items 513 and 523 do show data features expected from a vertical UXO: relatively high ELF values and ETO's similar to the pass orientation, as noted in the blind processing/ classification information included in Appendix D.

In Table 5, quite a few targets actually have quite good linearity, that is, high values in the last three columns. Interestingly, nine of these objects were rejected because of the varying (inconsistent) ETO estimated from different passes under the **Rule D** in Figure 5 (see Blind Processing/Classification Note in Appendix D). Two factors that could cause this situation are : (1) clustered UXO-like items, and (2) combined effect of position offset and vertical inclination. Factor (1) could be easily verified by the

GPS position information from the ground truth. Factor (2) could be verified if the GPR positions were recorded with an accurate GPS system and then compared with the target's GPS locations. At this time, insufficient information is available to us to evaluate either factor. The signal-to-clutter ratio of the responses from items 494 and 510 were too poor for positive identification. Item 494 seems to suffer from interference by some sort of underground layer scattering, as shown in Figure 16.

Table 7 lists findings for the rest of the missed UXO-like items. The responses of Item 502 suffer from interference with reflections from nearby targets, as demonstrated in Figure 13. This is due to closely clustered targets. Figure 14 and Figure 15 display a couple more examples of similar interference problems observed at Items 563 and 523. The presence of nearby target may not always be catastrophic for processing because, with multiple passes, sometimes a pass from a one orientation may produce better separation of individual responses and thus allow some degree of classification. Overall, however, clustered targets do complicate, and largely undercut the utility of multi-pass measurements for classification improvement.

Table 5. List of Missed UXO Items from Round-2 Classification Results, ANG (V) = inclination angle relative to the horiztontal (deg)

TAR #	Type	ANG (V)	GPR ID Round 1	GPR ID Round 2	CONF	true length (in)	ETL (in)	true depth (in)	DEP (in)	ELF	frequency ELF	early-time ELF
312	105mm Projectile	0	0	0	H	17	15	24	33	0.95	0.90	0.85
328	Signal Flare	114	0	0	L	10	11	1	6	0.92	0.94	0.83
330	2.36-inch Rocket	187	0	0	H	20	14	3	22	1.00	1.00	0.93
333	60mm Projectile	0	1	0	L	7	7	36	33	0.86	0.77	0.44
348	105mm Projectile	0	0	0	L	17	20	36	41	0.86	0.91	0.53
489	81mm Projectile	0	0	0	M	11	9	36	42	0.94	0.96	0.41
497	90mm Projectile	0	1	0	L	10	5	36	19	0.95	0.92	0.63
508	90mm Projectile	0	0	0	M	10	15	24	21	0.80	0.85	0.81
509	Stokes Mortar	194	0	0	H	14	15	13	25	0.99	0.93	0.97
367	Fragment	-999	0	0	L	8	10	18	17	0.23	0.89	0.96
494	105mm Projectile	0	0	0	L	17	16	48	26	0.94	0.25	0.73
510	Stokes Mortar	0	0	0	L	14	19	48	50	0.91	0.80	0.53
472	90mm Projectile	206	0	0	H	10	12	12	8	0.57	0.08	0.21
363	155mm Projectile	0	0	0	M	27	21	54	48	0.50	0.36	0.87
502	75mm Projectile	119	0	0	L	11	10	32	36	0.49	0.60	0.71
317	60mm Projectile	0	0	0	L	7	8	18	18	0.28	0.19	0.53
475	37mm Projectile	146	0	0	H	5	16	13	10	0.25	0.33	0.18
513	37mm Projectile	90	0	0	L	5	6	30	31	0.80	0.99	0.40
336	90mm Projectile	90	0	0	L	10	18	36	33	0.18	0.03	0.53
532	155mm Projectile	90	0	0	L	27	17	48	60	0.64	0.52	0.43
356	81mm Projectile	90	0	0	L	11	13	48	60	0.24	0.39	0.67
462	90mm Projectile	90	0	0	L	10	12	48	5	0.23	0.40	0.47
523	90mm Projectile	96	0	0	L	10	18	27	43	0.70	0.71	0.57
458	Fragment	-999	0	0	H	8	10	17	7	0.36	0.61	0.29

Table 6 List of Near Vertical UXO-Like Items

TAR #	Type	ANG (V)	True Depth (cm)	DEP	ELF	FELF	EELF
479	75mm Projectile	82	8	16	0.98	0.96	0.13
368	Other Debris	90	7	24	0.96	0.96	0.86
470	3.5-inch Rocket	90	16	41	0.98	0.95	0.75
471	105mm Projectile	90	24	48	0.98	0.97	0.82
478	81mm Projectile	90	24	22	0.79	0.88	0.61
482	60mm Projectile	90	24	30	0.92	0.76	0.56
513	37mm Projectile	90	30	31	0.80	0.99	0.40
341	81mm Illumination	90	36	27	0.70	0.77	0.45
336	90mm Projectile	90	36	33	0.18	0.03	0.53
345	105mm Projectile	90	48	6	0.68	0.66	0.62
532	155mm Projectile	90	48	60	0.64	0.52	0.43
356	81mm Projectile	90	48	60	0.24	0.39	0.67
462	90mm Projectile	90	48	5	0.23	0.40	0.47
381	Stokes Mortar	90	55	31	0.83	0.86	0.32
523	90mm Projectile	96	27	43	0.70	0.71	0.57
485	M9 Rifle Grenade	265	15	21	0.97	0.98	0.75

Table 7. Causes for Miscellaneous Missed UXOs

TAR #	Type	depth (in)	L (in)	D (in)	ANG (H)	ANG (V)	Conf	Round 1 Note	Round 2 Note	Finding
472	90mm Projectile	12	10	3.5	184	206	H	H. Plate, ETO~320	H. Plate, ETO~320	Did have consistent ETO but has scattering feature of a tilted plate RULE C in Figure 5
363	155mm Projectile	54	26.9	6.1	225	0	M			Pass 149,263 &31 Tilted UXO w/ varying ETO (149-100,263-0,31-0), Pass 3 Non UXO
502	75mm Projectile	32	11	3	244	119	L	UXO & tilted UXO w/ varying ETO		severe interference from nearby two objects
317	60mm Projectile	18	7	2.36	288	0	L	Poor SCR, Late-time contaminated		Low ELF at center, poor SCR due to contamination
475	37mm Projectile	13	4.5	1.46	210	146	H	Shallow Plate		Poor SCR, High-Pass filter yield Tilted UXO-like (L) R24in 178-deg. Pass.
458	Fragment	17	8	1			H	Shallow Plate		plate, with resonance in S11 on first pass and S22 on second pass

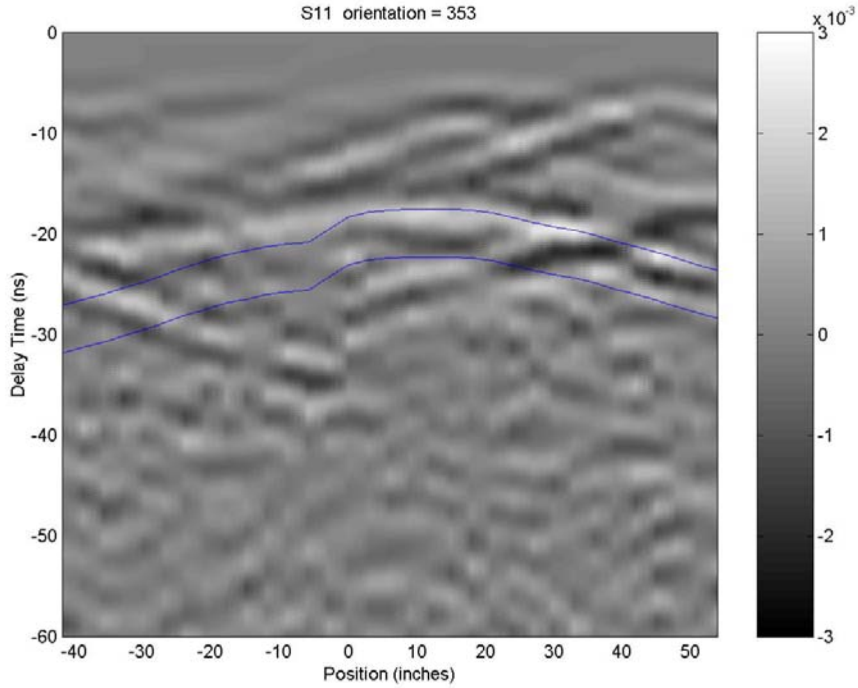

Figure 13. GPR scan data for Item 502 reveals interference from two nearby targets, with actual target response outlined in blue.

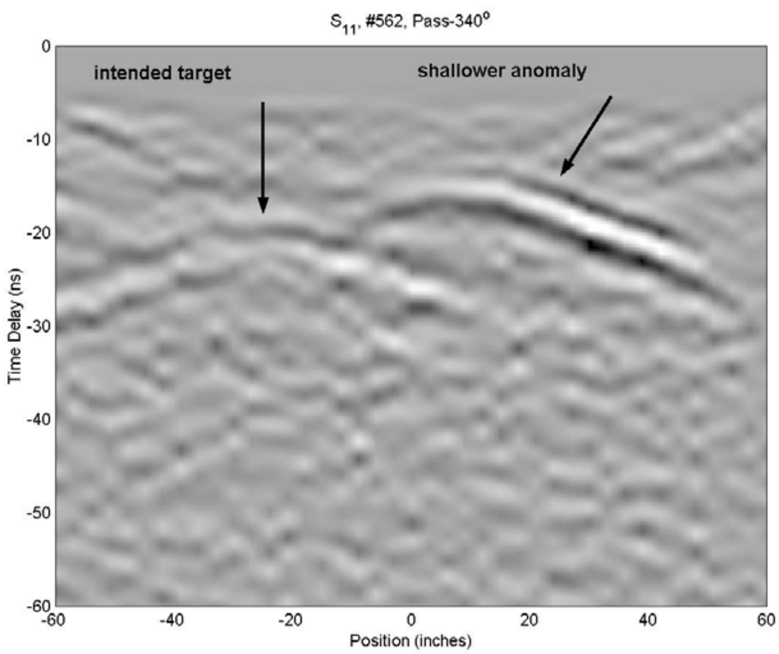

Figure 14. GPR scan data for Item 563 reveals interference from a stronger and shallower target.

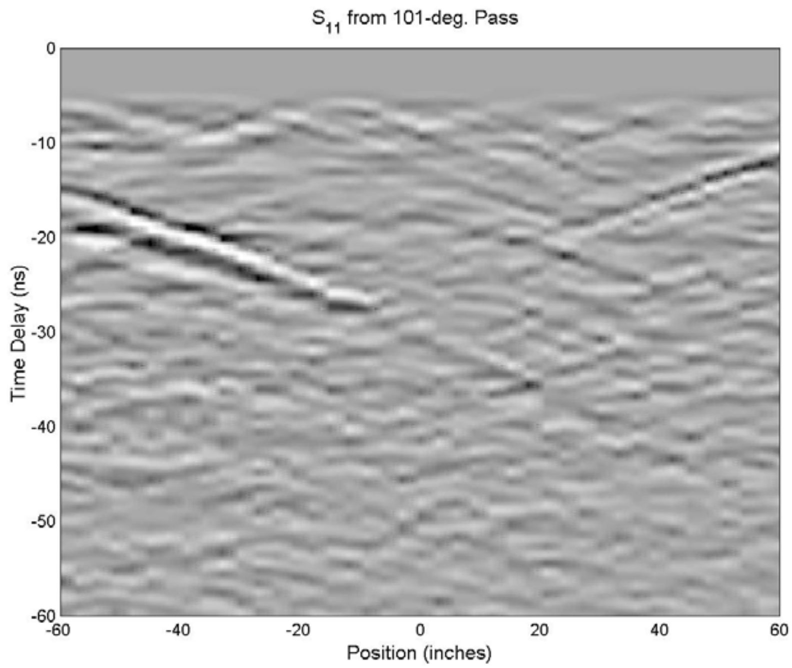

Figure 15. GPR scan data for Item 523 reveals interference from two nearby targets, on right and left. Intended target responses should be located near the center of the scan.

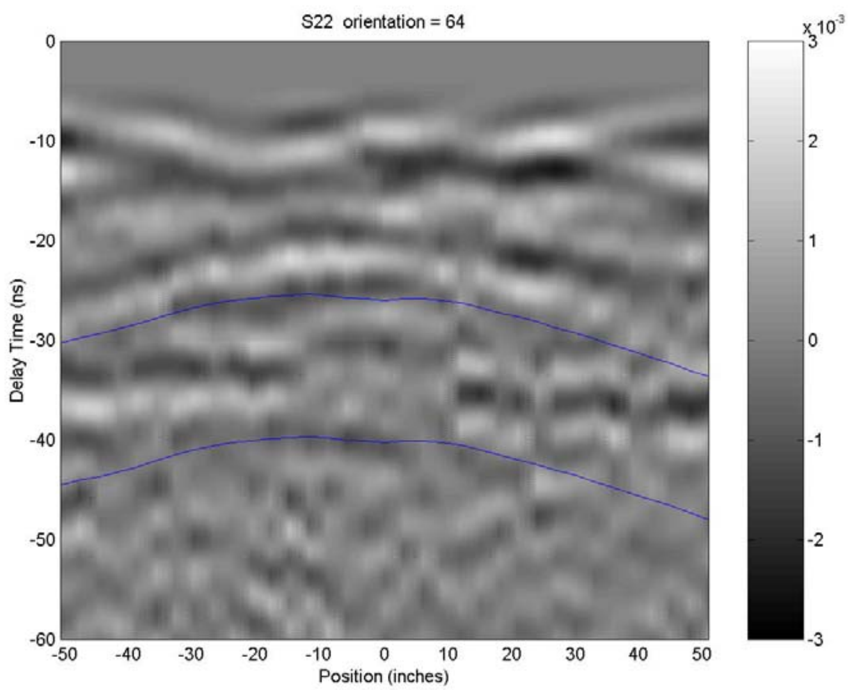

Figure 16. GPR data for Item 494, with interference from subsurface layer.

Causes of False Alarms and Discussion of Missed UXO

Table 8 lists the false alarm items in the Round-2 classification, based on the UXO-LIKE criterion. This includes all confidence levels of items that were identified as UXO-like. Eight objects out of the total 27 non-UXO-like objects produced false alarms. However, these include two MKII hand grenades! This type of grenade was designated as non-UXO-like because of its low L/D ratio. Two empty holes were classified as UXO-like; features for item 335 were actually not associated with the hole itself but with some other clutter phenomenon from a deeper region. The license plate was found to show very good UXO-like features, with only slight change in ETO's between passes. Hole 383 showed good linearity in its response but produced a varying ETO. The "hot rock" (376) also showed good linearity but the ETO varied from pass to pass (see Appendix D). Thus these two might have been ruled out as UXO under stricter criteria. At the same time, recall that some missed UXO-like items discussed above also have high ELF values but changing ETO's extracted from different passes. They were ruled out as UXO because of the unreliable ETO determination. Further examination of the Processing/Classification Notes in Appendix D reveals a major difference between those missed UXO-like items and the false alarm items. In particular, almost all of those missed UXO items showed magnetic dipole behavior in the handheld magnetometer (see the last column of Appendix D). Both the "hot rock" and empty hole showed no such magnetic dipole behavior. Thus combination of data from multiple sensors might have produced correct classification in these cases. Item 339 was actually ruled to be a horseshoe like object (see Appendix D) because of strong cross-polarized response in all passes. Its ETOs are also aligned with the pass orientations (Rule D of Figure 5). This item should have been classified as a non-UXO (late-night human error?). Item 305 is shaped like a small bent UXO-like object (see Appendix B.2) and showed some linear features but had poor signal-to-clutter ratio. That was why it was assigned a low confidence level.

Table 8. List of False Alarm Items During the Round 2 Based on "UXO-Like" Criterion

TAR #	Type	ANG (V)	CONF	true length (in)	ETL (in)	true depth (in)	DEP (in)	ELF	frequency ELF	early-time ELF
383	Empty Hole	-999	H		21	22	41	0.92	0.98	0.93
459	License Plate		H	12	15	17	22	0.91	0.91	0.82
339	Other Debris		H		11	3	12	0.50	0.65	0.55
376	Hot Rock	-999	M		11	24	28	0.98	0.88	0.95
340	Grenade MKII	89	M	5	6	11	4	0.97	0.98	0.73
320	Grenade MKII	0	L	5	4	2	2	0.83	0.82	0.48
305	Fragment	-999	L	3	6	7	8	0.81	0.94	0.48
335	Empty Hole	-999	L		7	6	44	0.64	0.60	0.32

Chapter 4 Conclusions

The first important finding from the Fort Ord demo is that, as in the previous demos, the system exhibits significant classification capability relative to random assignment of target identity at "hot spots." The blind classification performance based on the qualitative multiple-pass ELF, ETO and scattering pattering features shown in Figure 5, is consistent with the previous JPG V demo despite the significant differences in environmental conditions and targets distribution. While the Ft Ord soil and its condition were, in themselves, much more benign than at JPG , at Ft Ord the tunnel networks created by the local animals raised the clutter level of the site. The additional scattering from the tunnels of various sizes reduced the effective radar sensitivity and its effectiveness for detecting and classifying small UXO-like objects. The linearly polarized nature of the scattered fields generated by tunnels with small diameters relative to the wavelength could have confused the orientations of the intended UXO-like object that have comparable or weaker responses compared to responses from tunnels due to greater depths. This would result in a processing decision to drop a UXO-like object because of the inconsistent ETO's extracted from different passes. This type of linearly polarized tunnel responses could also have contributed to one false alarm from an empty site.

Another important target arrangement feature that made the Fort Ord site different and more challenging than the previous sites is target clustering. There were several groups of targets with two to four closely spaced items (1 to 3 feet apart). Measurement examples of the resulting interference effects were shown for several targets. The presence of interference hinders utilization of multiple-pass information to improve the classification accuracy.

Results show only a little change in classification statistics between the Round-1 (blind) and Round-2 (utilizing more accurate depth information). This is slightly different from the JPG V case, where improvement was observed in Round-2 classification. This could be because signal fading due to soil absorption was a major problem at JPG, making it difficult to distinguish target responses from those of ambient clutter sources (e.g. soil disturbance). Additional depth information allowed us to zero in on the correct depth/time range. However, in the dry sandy soil of Ft Ord, the main difficulty in identifying the target locale in the signals was inherent clutter due to subsurface structures.

A significant number of UXO-like objects were missed at Ft Ord not due to poor linear polarization features in the late time data, but because their ETO varied from pass to pass. This was

probably caused by scattering from tunnels and by interference form nearby targets when they were clustered. It could also be caused by the combination of significant inclination together with position offset, affecting the 3-D view of a linear object. Such a 3-D oblique view would result in the varying orientations we observed, when the orientation is projected on to the 2D antenna aperture plane. This might be addressed in the future by a combination of better target positioning (more accurate flagging), and also taking of GPR data over an entire areal grid over the target, with a faster system. Such a faster system is definitely possible.

The results here provide a strong argument for multi-sensor surveying. While the greatest failure in the GPR classifications constituted missed UXO's, examination of the data suggests that this might be avoided by inclusion of magnetometry or electromagnetic induction data. For example, the ROC curve in Figure 7 for the UXO-like criterion begins very well, rising quickly to about a 50% detection rate at about a 10% false alarm rate. However, further loosening the threshold criteria fails to pick up many of the remaining UXO-like objects very quickly, relative to the rate of increase in false alarms. Greater sophistication in the more inclusive decision criteria is in order. To this end, note that most of the missed UXO-like objects showed magnetic dipole behavior when pre-surveyed, even with a relatively crude handheld device. This makes them different from many false alarm objects that also show good linear features in the data but varying ETO. If the evidence of a magnetic dipole under this scenario were added as an indication of UXO-like target, most of these missed UXO's would have been correctly identified. Certainly, this requires further validation. Taking a 2-D grid data and a more sophisticated 3-D orientation-fitting model might improve the situation. A better approach is to improve the position accuracy based on magnetometer or EMI maps and some developed 3-D magnetic dipole fitting algorithm. Similar recommendations can be made for better estimation of the initial magnetic dipole orientation. Good initial position and orientation estimations by other systems would greatly improve the efficiency and accuracy of the GPR UXO classification.

Classifying objects as UXO-LIKE (as opposed to TRUE UXO) provides a fair test of the objectives of the processing system, which is based on distinguishing elongated objects from those that are not orientable. It also has some cogency as a means of comparison, if one considers that any other sensor system detecting similar target aspect ratios would make the same dig/no-dig recommendations. Ideally, however, one would like to be able to discriminate true UXO even from elongated fragments with lengths comparable to possible UXO. This requires the capability to determine the cross sectional area or to determine the 3-D scattering pattern, for separating an elongated, plate-like fragment from a cylinder-like UXO. The ramp profiling technique [7][8] has a potential for achieving the former. The latter

requires a fast radar system or an array system to collect 2-D backscattering or bi-static scattering patterns that can be used to infer the target's 3D geometry. Further, recent progress in interpreting broadband electromagnetic induction (EMI) responses of metal objects suggests that target aspect ratios might be estimated from EMI data [9]. Combined with length information from GPR, this would allow inference of general target dimensions.

APPENDICES

Appendix A GPR UXO Classification Tables

Definition of abbreviations used in the following tables:

True ID	UXO designation based on true UXO types: (1) UXO (0) non-UXO
UXO-LIKE ID	UXO designation based on UXO-like geometry (L/D>3) and operational frequency range (L>5”): (1) UXO (0) non-UXO
GPR ID	UXO designation based on GPR features: (1) UXO (0) non-UXO
Confidence Level	(H) high confidence (M) moderate confidence (L) low confidence.
ETO	**E**stimate **T**arget **O**rientation (azimuth).
CNR (NP/ns)	damping factor of the **C**omplex **N**atural **R**esonance.
CNR (GHz)	resonant frequency of the **C**omplex **N**atural **R**esonance.
ETL	**E**stimate **T**arget **L**ength.
DEP	estimate target **DEP**th.
Late-Time ELF(t)	**E**stimate **L**inear **F**actor extracted from late-time ***Time-Domain*** response.
Late-Time ELF(f)	**E**stimate **L**inear **F**actor extracted from late-time ***Frequency-Domain*** spectrum.
Early-time ELF	**E**stimate Linear **F**actor extracted form ***Early-Time*** response.

These classification (dig) lists are prioritized using the following order for items classified as UXO in the 1st Round, i.e. completely blind.

Confidence Level (H-M-L)-> ELF (high to low)-> FELF (high to low) -> EELF (high to low)

For items classified as non-UXO in the 1st Round, the following prioritization order is adopted:

Confidence Level (H-M-L)-> ELF (high to low)-> FELF (high to low) -> EELF (high to low)

Table 9. GPR Classification Results using "True UXO" Criteria.

Round 1 – w/o True Depth Feedback, Round 2 w/ True Depth Feedback

TAR #	Type	ANG (V)	offset_in	TRUE ID	GPR ID Round 1	GPR ID Round 2	Conf.	ANG (H)	ETO Deg.	length (inch)	ETL (in)	depth (inch)	DEP (in)	ELF	FELF	EELF
526	3.5-inch Rocket	151	2 NW	1	1	1	H	307	119	24	19	11	17	1.00	0.99	0.81
382	3.5-inch Rocket	311	12 NW	1	1	1	H	50	6	24	22	14	36	0.99	1.00	0.91
338	155mm Projectile	0	10 NW	1	1	1	H	59	-156	27	30	36	57	0.99	0.98	0.82
389	3.5-inch Rocket	30	6 W	1	1	1	H	340	95	24	24	24	30	0.98	0.99	0.80
470	3.5-inch Rocket	90	4 W	1	1	1	H	283	59	24	17	16	41	0.98	0.95	0.75
304	90mm Projectile	0	0	1	1	1	H	94	-78	10	16	1	12	0.98	0.94	0.48
471	105mm Projectile	90	6 N	1	1	1	H		-129	17	12	24	48	0.98	0.97	0.82
479	75mm Projectile	82	3 N	1	1	1	H	276	44	11	15	8	16	0.98	0.96	0.13
485	M9 Rifle Grenade	265	4 S	1	1	1	H	321	-140	4	11	15	21	0.97	0.98	0.75
326	81mm Illumination	0	0	1	1	1	H	139	109	25	25	36	55	0.96	0.89	0.85
359	Signal Illumination Flare	0	2 W	1	1	1	H	46	0	10	10	18	24	0.95	0.98	0.72
372	Stokes Mortar	36	0	1	1	1	H	193	155	14	16	34	38	0.95	1.00	0.88
536	81mm Projectile	0	6 W	1	1	1	H	351	159	11	12	18	27	0.94	0.95	0.75
353	Stokes Mortar	172	0	1	1	1	H	328	126	14	16	15	29	0.92	0.96	0.69
361	90mm Projectile	324	4 NW	1	1	1	H	169	126	10	11	12	16	0.90	0.95	0.58
308	3.5-inch Rocket	0	0	1	1	1	H	61	-153	24	27	36	55	0.88	0.87	0.42
307	81mm Illumination	0	1 E	1	1	1	H	315	116	25	22	24	38	0.86	0.97	0.62
391	90mm Projectile	192	0	1	1	1	H	120	106	10	16	30	41	0.83	0.78	0.55
324	75mm Projectile	0	6 E	1	1	1	H	51	-120	11	11	30	25	0.82	0.78	0.78
539	90mm Projectile	60	3 E	1	1	1	H	215	137	10	10	33	50	0.80	0.95	0.63
490	3.5-inch Rocket	0	3 W	1	1	1	H	195	11	24	13	12	19	0.79	0.95	0.93
478	81mm Projectile	90	6 E	1	1	1	H		41	11	12	24	22	0.79	0.88	0.61
322	M9 Rifle Grenade	229	6 W	1	1	1	H	239	34	4	12	12	19	0.71	0.88	0.76
474	Stokes Mortar	231	7 E	1	1	1	H	196	-141	14	15	33	38	0.68	0.75	0.80
390	Stokes Mortar	30	4 E	1	1	1	H	189	-94	14	15	27	30	0.67	0.82	0.82
501	2.36-inch Rocket	351	0	1	1	1	H	280	111	20	12	23	32	0.29	0.92	0.91
487	Stokes Mortar		8 SE	1	1	1	M	257	-115	14	15	40	41	0.99	0.95	0.53
331	90mm Projectile	0	0	1	1	1	M	175	152	10	12	2	2	0.98	0.99	0.59
482	60mm Projectile	90	0	1	1	1	M		67	7	10	24	30	0.92	0.76	0.56
319	90mm Projectile	0	8 N	1	1	1	M	258	-159	10	10	31	33	0.57	0.73	0.77
504	90mm Projectile	0	5 E	1	1	1	M	152	-70	10	11	48	53	0.43	0.61	0.59
497	90mm Projectile	0	2 S	1	1	0	L	269	-135	10	5	36	19	0.95	0.92	0.63
535	75mm Projectile	175	3 E	1	1	1	L	252	32	11	12	34	44	0.90	0.83	0.69
333	60mm Projectile	0	12 S	1	1	0	L	216	-48	7	7	36	33	0.86	0.77	0.44
320	Grenade MKII	0	0	1	1	1	L	232	40	5	4	2	2	0.83	0.82	0.48
332	60mm Projectile	0	8 NW	1	1	1	L	182	56	7	10	24	22	0.80	0.81	0.63
477	Stokes Mortar	0	12 NW	1	1	1	L	96	9	14	20	61	45	0.46	0.66	0.49
494	105mm Projectile	0	7 NE	1	0	0	L	338	-71	17	16	48	26	0.94	0.25	0.73
328	Signal Flare	114	0	1	0	0	L	299	-92	10	11	1	6	0.92	0.94	0.83
510	Stokes Mortar	0	6 E	1	0	0	L	89	-6	14	19	48	50	0.91	0.80	0.53
348	105mm Projectile	0	2 N	1	0	0	L	200	-162	17	20	36	41	0.86	0.91	0.53
521	90mm Projectile	106	4 S	1	0	1	L	112	-15	10	11	36	32	0.83	0.92	0.53
513	37mm Projectile	90	0	1	0	0	L		-108	5	6	30	31	0.80	0.99	0.40
523	90mm Projectile	96	9 S	1	0	0	L	155	103	10	18	27	43	0.70	0.71	0.57
341	81mm Illumination	90	5 E	1	0	1	L		-149	25	8	36	27	0.70	0.77	0.45
532	155mm Projectile	90	7 N	1	0	0	L		52	27	17	48	60	0.64	0.52	0.43
502	75mm Projectile	119	8 W	1	0	0	L	244	-94	11	10	32	36	0.49	0.60	0.71
317	60mm Projectile	0	10 S	1	0	0	L	288	83	7	8	18	18	0.28	0.19	0.53
370	Grenade MKII	90	6 SE	1	0	0	L		55	5	7	6	6	0.26	0.25	0.21
356	81mm Projectile	90	7 N	1	0	0	L		-160	11	13	48	60	0.24	0.39	0.67
462	90mm Projectile	90	6 E	1	0	0	L		-43	10	12	48	5	0.23	0.40	0.47
336	90mm Projectile	90	0	1	0	0	L		-52	10	18	36	33	0.18	0.03	0.53
340	Grenade MKII	89	2 N	1	0	1	M	29	-114	5	6	11	4	0.97	0.98	0.73
489	81mm Projectile	0	5 S	1	0	0	M	256	-53	11	9	36	42	0.94	0.96	0.41
381	Stokes Mortar	90	8 SW	1	0	1	M		-130	14	18	55	31	0.83	0.86	0.32
508	90mm Projectile	0	10 N	1	0	0	M	140	-88	10	15	24	21	0.80	0.85	0.81

TAR #	Type	ANG (V)	offset_in	TRUE ID	GPR ID Round 1	GPR ID Round 2	Conf.	ANG (H)	ETO Deg.	length (inch)	ETL (in)	depth (inch)	DEP (in)	ELF	FELF	EELF
345	105mm Projectile	90	14 E	1	0	1	M		42	17	16	48	6	0.68	0.66	0.62
363	155mm Projectile	0	12 E	1	0	0	M	225	-64	27	21	54	48	0.50	0.36	0.87
330	2.36-inch Rocket	187	6 NW	1	0	0	H	14	-88	20	14	3	22	1.00	1.00	0.93
509	Stokes Mortar	194	1 W	1	0	0	H	355	103	14	15	13	25	0.99	0.93	0.97
312	105mm Projectile	0	9 SW	1	0	0	H	103	128	17	15	24	33	0.95	0.90	0.85
472	90mm Projectile	206	4 E	1	0	0	H	184	-44	10	12	12	8	0.57	0.08	0.21
475	37mm Projectile	146	0	1	0	0	H	210	177	5	16	13	10	0.25	0.33	0.18
366	Other Debris		5 W	0	1	1	H		-68		26	24	34	1.00	0.98	0.65
460	Fragment	-999	0	0	1	1	H	-999	-142	12	16	17	25	0.97	0.92	0.87
368	Other Debris	90	2 S	0	1	1	H		-103		25	7	24	0.96	0.96	0.86
483	Fragment	-999	0	0	1	1	H	-999	-37	6	7	4	12	0.93	0.97	0.24
383	Empty Hole	-999	12 E	0	1	1	H	-999	-29		21	22	41	0.92	0.98	0.93
459	Other Debris		4 SW	0	1	1	H		-150		15	17	22	0.91	0.91	0.82
531	Fragment	-999	1 N	0	1	1	H	-999	152	7	6	4	9	0.89	0.94	0.89
318	Other Debris	-999	4 SE	0	1	1	H	-999	1		25	22	39	0.78	0.87	0.82
376	Hot Rock	-999	4 NE	0	1	1	M		-61		11	24	28	0.98	0.88	0.95
394	Fragment	-999	5 NW	0	1	0	M	-999	-86	5	4	7	18	0.25	0.28	0.57
347	Fragment	-999	0	0	1	1	L		-39	5	6	6	9	1.00	1.00	0.81
305	Fragment	-999	4 SE	0	1	1	L		-74	3	6	7	8	0.81	0.94	0.48
545	Fragment	-999	2 NE	0	1	1	L	-999	-53	6	7	9	12	0.69	0.87	0.75
335	Empty Hole	-999	4 E	0	1	1	L	-999	116		7	6	44	0.64	0.60	0.32
364	Fragment	-999	1 N	0	1	0	L	-999	-109	3	7	17	36	0.45	0.37	0.25
358	Fragment	-999	0	0	1	0	L	-999	-159	4	14	1	12	0.23	0.11	0.17
395	Fragment	-999	0	0	0	0	L	-999	-9	3	4	10	9	NaN	0.49	0.55
473	Hot Rock		8 SW	0	0	0	L		2		17	20	33	0.79	0.79	0.74
457	Hot Rock		2 S	0	0	0	L		64		15	4	47	0.76	0.49	0.27
500	Fragment	-999	6 E	0	0	0	L	-999	-79	4	4	2	7	0.74	0.52	0.43
306	Fragment	-999	7 NE	0	0	0	L		12	4	10	12	46	0.73	0.81	0.36
396	Fragment	-999	5 SE	0	0	0	L	-999	82	5	6	6	40	0.56	0.56	0.47
520	Other Debris		2 N	0	0	0	L		173		6	6	14	0.54	0.40	0.64
540	Hot Rock		0	0	0	0	L		154		12	1	54	0.46	0.51	0.63
377	Other Debris	-999	0	0	0	0	L	-999	84		5	16	19	0.39	0.36	0.41
463	Other Debris		1 W	0	0	0	L		134		6	13	15	0.24	0.43	0.66
367	Fragment	-999	4 N	0	0	0	L	-999	-169	8	10	18	17	0.23	0.89	0.96
527	Other Debris		0	0	0	0	L		131		4	1	10	0.10	0.04	0.33
315	Other Debris	-999	5 E	0	0	0	M		166		10	12	59	0.65	0.96	0.72
464	Other Debris		2 N	0	0	0	M		-22		5	9	13	0.32	0.37	0.24
339	Other Debris		3 S	0	0	1	H		75		11	3	12	0.50	0.65	0.55
481	Other Debris		0	0	0	0	H		-149		19	2	7	0.44	0.45	0.11
458	Fragment	-999	3 N	0	0	0	H	-999	-42	8	10	17	7	0.36	0.61	0.29
543	Fragment	-999	4 E	0	0	0	H	-999	-8	4	19	23	42	0.23	0.12	0.40

Table 10. GPR Classification Results using "UXO-Like" Criteria (L/D>3 and L>5").

Round 1 – w/o True Depth Feedback, Round 2 w/ True Depth Feedback

TAR #	Type	ANG (V)	offset in	UXO-LIKE ID	GPR ID Round 1	GPR ID Round 2	CONF	true azi. (deg)	ETO Deg.	true length (in)	ETL (in)	true depth (in)	DEP (in)	ELF	frequency ELF	early-time ELF
366	Other Debris		5 W	1	1	1	H		-68	24	26	24	34	1.00	0.98	0.65
526	3.5-inch Rocket	151	2 NW	1	1	1	H	307	119	24	19	11	17	1.00	0.99	0.81
382	3.5-inch Rocket	311	12 NW	1	1	1	H	50	6	24	22	14	36	0.99	1.00	0.91
338	155mm Projectile	0	10 NW	1	1	1	H	59	-156	27	30	36	57	0.99	0.98	0.82
389	3.5-inch Rocket	30	6 W	1	1	1	H	340	95	24	24	24	30	0.98	0.99	0.80
470	3.5-inch Rocket	90	4 W	1	1	1	H	283	59	24	17	16	41	0.98	0.95	0.75
304	90mm Projectile	0	0	1	1	1	H	94	-78	10	16	1	12	0.98	0.94	0.48
471	105mm Projectile	90	6 N	1	1	1	H		-129	17	12	24	48	0.98	0.97	0.82
479	75mm Projectile	82	3 N	1	1	1	H	276	44	11	15	8	16	0.98	0.96	0.13
460	Fragment	-999	0	1	1	1	H	-999	-142	12	16	17	25	0.97	0.92	0.87
485	M9 Rifle Grenade	265	4 S	1	1	1	H	321	-140	4	11	15	21	0.97	0.98	0.75
368	Other Debris	90	2 S	1	1	1	H		-103	18	25	7	24	0.96	0.96	0.86
326	81mm Illumination	0	0	1	1	1	H	139	109	25	25	36	55	0.96	0.89	0.85
359	Signal Illumination Flare	0	2 W	1	1	1	H	46	0	10	10	18	24	0.95	0.98	0.72
372	Stokes Mortar	36	0	1	1	1	H	193	155	14	16	34	38	0.95	1.00	0.88
536	81mm Projectile	0	6 W	1	1	1	H	351	159	11	12	18	27	0.94	0.95	0.75
483	Fragment	-999	0	1	1	1	H	-999	-37	6	7	4	12	0.93	0.97	0.24
353	Stokes Mortar	172	0	1	1	1	H	328	126	14	16	15	29	0.92	0.96	0.69
361	90mm Projectile	324	4 NW	1	1	1	H	169	126	10	11	12	16	0.90	0.95	0.58
531	Fragment	-999	1 N	1	1	1	H	-999	152	7	6	4	9	0.89	0.94	0.89
308	3.5-inch Rocket	0	0	1	1	1	H	61	-153	24	27	36	55	0.88	0.87	0.42
307	81mm Illumination	0	1 E	1	1	1	H	315	116	25	22	24	38	0.86	0.97	0.62
391	90mm Projectile	192	0	1	1	1	H	120	106	10	16	30	41	0.83	0.78	0.55
324	75mm Projectile	0	6 E	1	1	1	H	51	-120	11	11	30	25	0.82	0.78	0.78
539	90mm Projectile	60	3 E	1	1	1	H	215	137	10	10	33	50	0.80	0.95	0.63
490	3.5-inch Rocket	0	3 W	1	1	1	H	195	11	24	13	12	19	0.79	0.95	0.93
478	81mm Projectile	90	6 E	1	1	1	H		41	11	12	24	22	0.79	0.88	0.61
318	Other Debris	-999	4 SE	1	1	1	H	-999	1	24	25	22	39	0.78	0.87	0.82
322	M9 Rifle Grenade	229	6 W	1	1	1	H	239	34	4	12	12	19	0.71	0.88	0.76
474	Stokes Mortar	231	7 E	1	1	1	H	196	-141	14	15	33	38	0.68	0.75	0.80
390	Stokes Mortar	30	4 E	1	1	1	H	189	-94	14	15	27	30	0.67	0.82	0.82
501	2.36-inch Rocket	351	0	1	1	1	H	280	111	20	12	23	32	0.29	0.92	0.91
487	Stokes Mortar		8 SE	1	1	1	M	257	-115	14	15	40	41	0.99	0.95	0.53
331	90mm Projectile	0	0	1	1	1	M	175	152	10	12	2	2	0.98	0.99	0.59
482	60mm Projectile	90	0	1	1	1	M		67	7	10	24	30	0.92	0.76	0.56
319	90mm Projectile	0	8 N	1	1	1	M	258	-159	10	10	31	33	0.57	0.73	0.77
504	90mm Projectile	0	5 E	1	1	1	M	152	-70	10	11	48	53	0.43	0.61	0.59
347	Fragment	-999	0	1	1	1	L		-39	5	6	6	9	1.00	1.00	0.81
497	90mm Projectile	0	2 S	1	1	0	L	269	-135	10	5	36	19	0.95	0.92	0.63
535	75mm Projectile	175	3 E	1	1	1	L	252	32	11	12	34	44	0.90	0.83	0.69
333	60mm Projectile	0	12 S	1	1	0	L	216	-48	7	7	36	33	0.86	0.77	0.44
332	60mm Projectile	0	8 NW	1	1	1	L	182	56	7	10	24	22	0.80	0.81	0.63
545	Fragment	-999	2 NE	1	1	1	L	-999	-53	6	7	9	12	0.69	0.87	0.75
477	Stokes Mortar	0	12 NW	1	1	1	L	96	9	14	20	61	45	0.46	0.66	0.49
494	105mm Projectile	0	7 NE	1	0	0	L	338	-71	17	16	48	26	0.94	0.25	0.73
328	Signal Flare	114	0	1	0	0	L	299	-92	10	11	1	6	0.92	0.94	0.83
510	Stokes Mortar	0	6 E	1	0	0	L	89	-6	14	19	48	50	0.91	0.80	0.53
348	105mm Projectile	0	2 N	1	0	0	L	200	-162	17	20	36	41	0.86	0.91	0.53
521	90mm Projectile	106	4 S	1	0	1	L	112	-15	10	11	36	32	0.83	0.92	0.53
513	37mm Projectile	90	0	1	0	0	L		-108	5	6	30	31	0.80	0.99	0.40
523	90mm Projectile	96	9 S	1	0	0	L	155	103	10	18	27	43	0.70	0.71	0.57

TAR #	Type	ANG (V)	offset in	UXO-LIKE ID	GPR ID Round 1	GPR ID Round 2	CONF	true azi. (deg)	ETO Deg.	true length (in)	ETL (in)	true depth (in)	DEP (in)	ELF	frequency ELF	early-time ELF
341	81mm Illumination	90	5 E	1	0	1	L		-149	25	8	36	27	0.70	0.77	0.45
532	155mm Projectile	90	7 N	1	0	0	L		52	27	17	48	60	0.64	0.52	0.43
502	75mm Projectile	119	8 W	1	0	0	L	244	-94	11	10	32	36	0.49	0.60	0.71
317	60mm Projectile	0	10 S	1	0	0	L	288	83	7	8	18	18	0.28	0.19	0.53
356	81mm Projectile	90	7 N	1	0	0	L		-160	11	13	48	60	0.24	0.39	0.67
462	90mm Projectile	90	6 E	1	0	0	L		-43	10	12	48	5	0.23	0.40	0.47
367	Fragment	-999	4 N	1	0	0	L	-999	-169	8	10	18	17	0.23	0.89	0.96
336	90mm Projectile	90	0	1	0	0	L		-52	10	18	36	33	0.18	0.03	0.53
489	81mm Projectile	0	5 S	1	0	0	M	256	-53	11	9	36	42	0.94	0.96	0.41
381	Stokes Mortar	90	8 SW	1	0	1	M		-130	14	18	55	31	0.83	0.86	0.32
508	90mm Projectile	0	10 N	1	0	0	M	140	-88	10	15	24	21	0.80	0.85	0.81
345	105mm Projectile	90	14 E	1	0	1	M		42	17	16	48	6	0.68	0.66	0.62
363	155mm Projectile	0	12 E	1	0	0	M	225	-64	27	21	54	48	0.50	0.36	0.87
330	2.36-inch Rocket	187	6 NW	1	0	0	H	14	-88	20	14	3	22	1.00	1.00	0.93
509	Stokes Mortar	194	1 W	1	0	0	H	355	103	14	15	13	25	0.99	0.93	0.97
312	105mm Projectile	0	9 SW	1	0	0	H	103	128	17	15	24	33	0.95	0.90	0.85
472	90mm Projectile	206	4 E	1	0	0	H	184	-44	10	12	12	8	0.57	0.08	0.21
458	Fragment	-999	3 N	1	0	0	H	-999	-42	8	10	17	7	0.36	0.61	0.29
475	37mm Projectile	146	0	1	0	0	H	210	177	5	16	13	10	0.25	0.33	0.18
383	Empty Hole	-999	12 E	0	1	1	H	-999	-29		21	22	41	0.92	0.98	0.93
459	Other Debris		4 SW	0	1	1	H		-150	12	15	17	22	0.91	0.91	0.82
376	Hot Rock	-999	4 NE	0	1	1	M		-61		11	24	28	0.98	0.88	0.95
394	Fragment	-999	5 NW	0	1	0	M	-999	-86	5	4	7	18	0.25	0.28	0.57
320	Grenade MKII	0	0	0	1	1	L	232	40	5	4	2	2	0.83	0.82	0.48
305	Fragment	-999	4 SE	0	1	1	L		-74	3	6	7	8	0.81	0.94	0.48
335	Empty Hole	-999	4 E	0	1	1	L	-999	116		7	6	44	0.64	0.60	0.32
364	Fragment	-999	1 N	0	1	0	L	-999	-109	3	7	17	36	0.45	0.37	0.25
358	Fragment	-999	0	0	1	0	L	-999	-159	4	14	1	12	0.23	0.11	0.17
370	Grenade MKII	90	6 SE	0	0	0	L		55	5	7	6	6	0.26	0.25	0.21
395	Fragment	-999	0	0	0	0	L	-999	-9	3	4	10	9	NaN	0.49	0.55
473	Hot Rock		8 SW	0	0	0	L		2		17	20	33	0.79	0.79	0.74
457	Hot Rock		2 S	0	0	0	L		64		15	4	47	0.76	0.49	0.27
500	Fragment	-999	6 E	0	0	0	L	-999	-79	4	4	2	7	0.74	0.52	0.43
306	Fragment	-999	7 NE	0	0	0	L		12	4	10	12	46	0.73	0.81	0.36
396	Fragment	-999	5 SE	0	0	0	L	-999	82	5	6	6	40	0.56	0.56	0.47
520	Other Debris		2 N	0	0	0	L		173		6	6	14	0.54	0.40	0.64
540	Hot Rock		0	0	0	0	L		154		12	1	54	0.46	0.51	0.63
377	Other Debris	-999	0	0	0	0	L	-999	84	4	5	16	19	0.39	0.36	0.41
463	Other Debris		1 W	0	0	0	L		134	4	6	13	15	0.24	0.43	0.66
527	Other Debris		0	0	0	0	L		131		4	1	10	0.10	0.04	0.33
340	Grenade MKII	89	2 N	0	0	1	M	29	-114	5	6	11	4	0.97	0.98	0.73
315	Other Debris	-999	5 E	0	0	0	M		166		10	12	59	0.65	0.96	0.72
464	Other Debris		2 N	0	0	0	M		-22	4	5	9	13	0.32	0.37	0.24
339	Other Debris		3 S	0	0	1	H		75		11	3	12	0.50	0.65	0.55
481	Other Debris		0	0	0	0	H		-149		19	2	7	0.44	0.45	0.11
543	Fragment	-999	4 E	0	0	0	H	-999	-8	4	19	23	42	0.23	0.12	0.40

Appendix B Pictures of Clutter Items

B.1 Pictures of "Other Debris" Items

ITEM 481

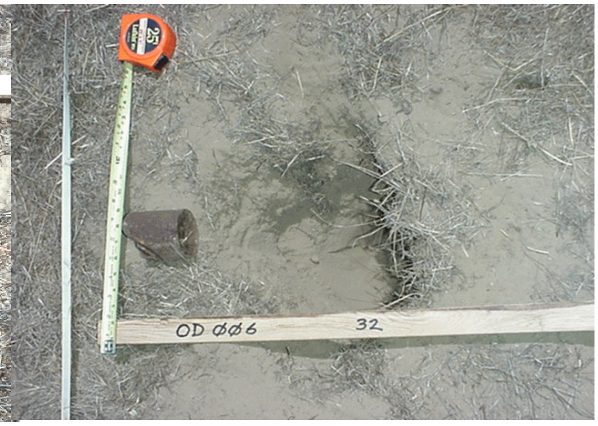

ITEM 377

ITEM 339

ITEM 520

ITEM 315

ITEM 366 (UXO-like)

ITEM 368 (UXO-like)

ITEM 527

ITEM 459

ITEM 318 (UXO-like)

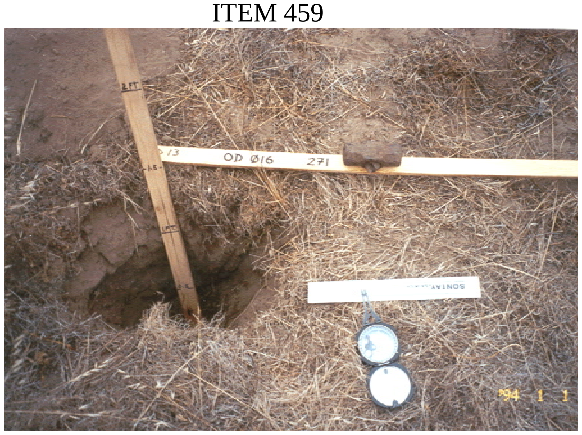

ITEM 463

ITEM 464

B.2 Pictures of "Fragments" Items

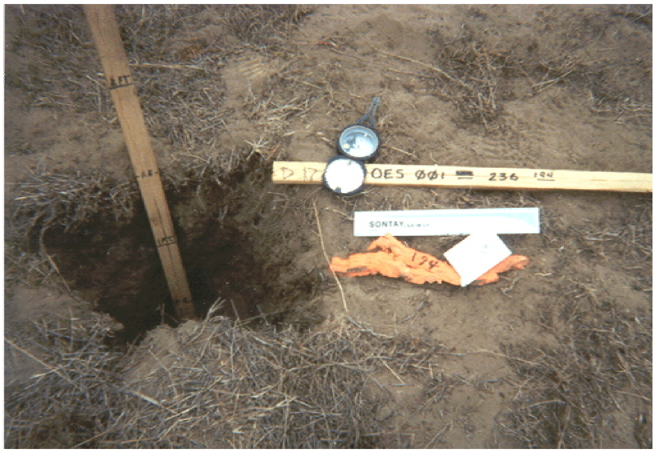

ITEM 460

ITEM 367

ITEM 483

ITEM 395

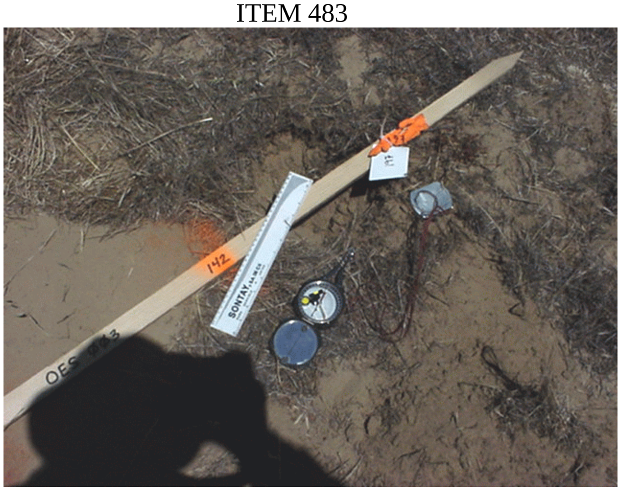

ITEM 394

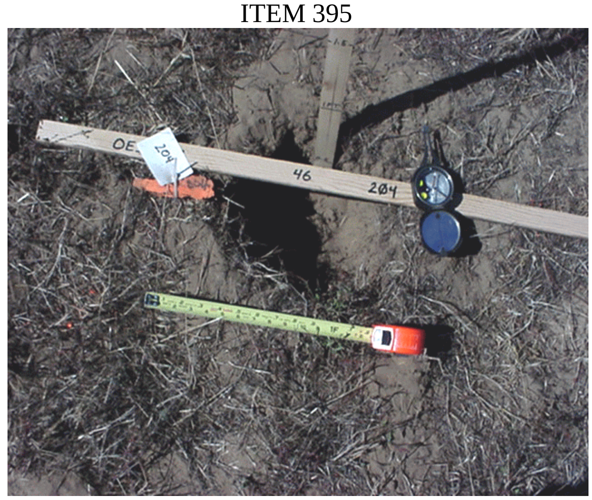

ITEM 347

ITEM 458

ITEM 306

ITEM 500

ITEM 396

ITEM 531

ITEM 545

ITEM 543

ITEM 305

ITEM 364

ITEM 358

Appendix C Archiving

GPR Data Files – *.cdt

The data for system-calibrated frequency-domain radar data was stored in ASCII-format files called “**aydddaa.cdt**”, where “a” is from A to Z for file ordering. The letter “y” indicates the last digit of the year. For example, “0” means the year of 2000. The three-digit number, “ddd” , indicates the Julian date when the data was stored. Each file contains two-dimensional data array for one target location. The first frequency (10 MHz) data was stored in the first row, the second frequency (12 MHz) data was stored in the second row, etc. Each column stores the frequency, co-polarization and cross-polarization data in a format shown below. For each radar "*.cdt” file, there is an associated comment file called “*.txt” to store the system information, comments and processed results. All of these files will be available in a CD-ROM after this submission of this report.

Frequency (MHz)	Re(S_{11})	Im(S_{11})	Re(S_{21})	Im(S_{21})	Re(S_{22})	Im(S_{22})

"Re()" and "Im()" indicate the real and imaginary parts, respectively (combined, these provide the amplitude and phase).

Comment Text Files - *.txt

The comment text files contain information about measurement conditions (i.e. position, direction, etc.) and any comments the user entered during the measurements. Comment files with an extra letter on the end of the names are the processed comment files. These files contain all the information about measurement, as before, but also contain information about the processing of the file. For example, the comment file a0014gbu.txt is printed below:

14-Jan-2000/Target #: 101/No Target File: a0014fz.cdt/Antenna Orientation: 194/Antenna Position: xoffset: 0.0000/yoffset: 10.0000/Relative Permittivity: 4/User Comments: UE3@@@/$ETO/3/ -1.0000/ 179.0000/ 0.7471/ELF/2/ 0.7726/ 0.0213/CNR/2/ 0.0913/ 0.2046/ETL/1/ 0.3666/SNR/1/ 49.7574/TCP/2/ 12.3932/ 0.5861/timerange1/ 17.3146/timerange2/ 24.4088/timepeakmax/ 12.3932/waveformselection/ 3.0000/FELF/ 0.8443/$$**

This is a typical comment file after processing. The letter ‘u’ on the end of the file name denotes that a user-specified center frequency band-pass filter was used before the processing of the file. A letter ‘f’ on the end would denote that the full 800 MHz bandwidth was used in processing that file, while a letter ‘l’ and ‘h’ denotes that a low-pass and a high-pass filter was used, respectively.

One can see that all of the processed parameters (i.e. ETO, ETL, ELF, etc.) for this target are stored in the file. There are also four other parameters (timerange1, timerange2, timepeakmax, and waveformselection) stored in the file, which provide information about the late-time region selected to do processing on. These parameters allow for the automatic re-processing of the data, if necessary.

Processed Files -*.mat Files

The processed data is saved in *.mat format (a Matlab file fomat), in which the following variables are saved.

Variables of Processed Data Results

ELF – Estimated Linear Factor vs. position
fELF – Frequency Estimated Linear Factor vs. position
melf – Mean of ELF and fELF
ETO – Estimated Target Orientation vs. position
CNR – Complex Natural Resonance and Damping vs. position
ETL – Estimated Target Length vs. position
Y1a – Position vector
SNR – Estimated Signal to Noise Ratio vs. position
SCR – Estimated Signal to Clutter Ratio vs. position
ATV – Antenna Orientation

Variables of How Data was Processed

SELECTION –Data Channel used for CNR extraction
ftype – Type of frequency domain filter
ucfreq2 – User Centered frequency for the adaptive bandpass filter
npoint – Number of points in the adaptive bandpass filter
nx – Position vector for late-time region selection
ntmax – First Time position for late-time region vs. x-position
numTdiff – Number of points in late-time region vs. x-postion
T0 – Variable for slope gain

TM – Variable for slope gain
gainfac – Variable for slope gain
imgT – Variable for adaptive smoothing
imgindT - Variable for adaptive smoothing
imgindx - Variable for adaptive smoothing
imgN - Variable for adaptive smoothing
SIDE - Variable for adaptive smoothing

Appendix D Blind Processing/Classification Note

No.	TAR.	Pass 1	Pass 2	Pass 3	Pass 4	General Comments	Proc. Note	GPR ID	Conf.	Best Pass ETO	Pass1 Feature Comments	Pass2 Feature Comments	Pass3 Feature Comments	
1	304	189	260	27			20"(-) ATV=225, ETO varies with ATV,Near Vertical UXO	1	H	189	V. Plate or Tilted UXO or offset Clutter	Offset, tilted UXO	Tilted UXO	
2	305	183	85	291				1	L	183	UXO-Like, ETO~105, POS=-10", Small & Shallow, Poor SCR,	ETO~80, Poor SCR	Shallow,Small, Poor SCR, UXO-Like X=10	
3	306	280	0			interfered	sign change in center	0	L	280	24ns, non-UXO, early-time	24ns,Non-UXO, early-time		
4	307	126	9					1	H	126	UXO-Like	UXO-Like		
5	308	176	251	208			Check Flag Proximitity (2 flags?)	1	H	208	Two Targets		Second UXO-Like, Separated 4', 45deg, Orthogonal	
6	312	240	25			L Shaped		0	H	25	ETO=56, UXO-Like	UXO-Like, ETO=133		
7	315	294	217	166				0	M	166	Strong CNR, UXO-like, ETO=52 (strong clutter)	Strong CNR, UXO-Like, ETO=0	Strong CNR, UXO-Like, ETO=166	
8	317	127	73			Poor SCR	15"(-) ATV1, 0.1~0.6GHz	0	L	127	LOW ELF Ctr. ETO~100, Late-Time Contaminated	Low ELF Ctr., ETO~70		
9	318	49	7				Good, < 0.4GHz	1	H	7	UXO-Like, ETO~20	UXO-Like, ETO~0		
10	319	122	207					1	M	207	UXO-Like, ETO~40	UXO-Like (-10"), ETO~20		
11	320	43	124					1	L	43	Shallow, Small, Non-UXO, ETO~40	Poor SCR, UXO-Like (-10") ETO~40		
12	322	147	41					1	H	41	UXO-like, ETO=60	UXO-like, ETO=40		
13	324	145	220					1	H	145	UXO-Like,ETO=60,2nd object 50" after	V. UXO, ETO=40		
14	326	336	83					1	H	336	Tilted UXO-Like, ETO~80	Poor-Resonant, ETO~60,		
15	328	65	178			Stange ETO? Bent bar		0	L	178	Tilted UXO-Like, ETO~34	UXO-Like, ETO=88		
16	330	334	140			Varying ETO, Bent Bar, shallow		0	H	140	UXO-Like, ETO=150	UXO-Like ETO=90		
17	331	193	287	152				1	M	152	Tilted UXO-like, ETO=130	Tilted, UXO-Like, ETO~105	UXO-Like, ETO=152	
18	332	65	324					1	L	324	UXO-Like, ETO=56, Poor SCR	Tilted UXO-Like, ETO=60, offset 20"		
19	333	67	232	322			10"(+) ATV=67	1	L	322	UXO-Like, Weak, ETO~162	UXO-Like, Weak,	V. UXO-Like, Weak,	

No.	TAR.	Pass 1	Pass 2	Pass 3	Pass 4	General Comments	Proc. Note	GPR ID	Conf.	Best Pass ETO	Pass1 Feature Comments	Pass2 Feature Comments	Pass3 Feature Comments	
												ETO~20	ETO~132	
20	335	15	94			V. UXO?		1	L	15	V. UXO-Like, ETO~13, Poor SCR	Weak or NO Target Response		
21	336	36	100	339		Poor SCR		0	L	339	V. UXO-Like, ETO~34, POS=-10", Poor SCR	Weak or NO Target Response	Non-UXO, ETO~155, POS=-20"	
22	338	195	103	232	193			1	H	103	UXO-Like, ETO=14	UXO-Like, ETO~24	UXO-Like,ETO~20	
23	339	230	33	84		Horseshoe Like (good Cross-Pol. In all Passes)		0	H	84	Non-UXO, ETO~40	Non-UXO, ETO=28	Non-UXO, ETO~80	
24	340	140	133	37			Good example of multiple targets	0	M	140	Shallow, Small, Non-UXO, Contain 339 Responses at Offset		Contaminated by TAR 339	
25	341	255	158	72				0	L	255	Non-UXO, Weak, Small, Poor SCR	Weak or NO Target Response	Weak or No Target Response	
26	345	295	42	298				0	M	42	Shallow Plate	Shallow Plate		
27	347	224	116	322		Small UXO-like		1	L	322		Tilted UXO-Like, ETO~30, Shallow, small, Poor SCR	Tilted UXO, ETO~40, Small	
28	348	120	200				Good	0	L	200	UXO-Like,ETO~75	UXO-Like, ETO~20, POS=5"		
29	353	150	35				10"(+) ATV1, good	1	H	35	Tilted UXO-Like, ETO~100	Tilted UXO-Like, ETO~125		
30	356	154	211	94			Deep	0	L	211	Weak or NO Target Response	Non-UXO, ETO~20, Deep, Poor SCR	Many Junks!, ETO~7, POS=--30"	
31	358	201	270	316		Many Clutter	10"(-) ATV1	1	L	201	Shallow UXO-Like	Deep, Poor SCR, V. UXO?	Deep, Poor SCR	
32	359	270	348				Good Shallow UXO-Like+Deep Anomaly	1	H	270	UXO-Like, ETO~0	UXO-Like, ETO=160		
33	361	127	134	15		20"(-) ATV=134	Good,Tilted	1	H	127	Tilted UXO-Like, ETO~127	Tilted UXO-Like, ETO~134	UXO-Like, ETO~110	
34	363	149	263	168	31	15"(+) ATV=149		0	M	168	Tilted UXO-Like, ETO~110	Tilted UXO-Like, ETO~0	Non-UXO, ETO~80, Plate	UXO-Like,ETO~0
35	364	157	205			20"(-) ATV=157		1	L	205	ETO~70, POS=10", Weak			
36	366	202	264				good	1	H	202	UXO-Like, ETO~112	UXO-Like, ETO~80		
37	367	148	99	25				0	L	99	UXO-Like, ETO~140	UXO-Like, ETO~20	UXO-Like, ETO~20	
38	368	257	160				Vertical UXO-Like	1	H	160	V. UXO-Like			
39	370	59	230	142				0	L	59	Near Surface Non-UXO		Near surface plate	
40	372	159	344					1	H	159	Tilted UXO, ETO~160	Tilted UXO, ETO~160		

No.	TAR.	Pass 1	Pass 2	Pass 3	Pass 4	General Comments	Proc. Note	GPR ID	Conf.	Best Pass ETO	Pass1 Feature Comments	Pass2 Feature Comments	Pass3 Feature Comments	
41	376	320	230	157			15"(-) ATV1	1	M	320	Tilted UXO, ETO~-60-0	Tilted UXO, ETO~3	UXO-Like, ETO~100	
42	377	321	203	79		Small		0	L	321	Non-UXO, ETO~80, Small, Shallow	Non-UXO, Small, Poor SCR	Poor SCR	
43	381	235	234	111	325	20"(+)ATV=234		0	M	235	Non-resonant plate POS=20", Weak or No		Non-UXO	
44	382	41	275			15"(-) ATV=41	Good,Tilted	1	H	275	Tilted UXO, ETO~40	UXO-Like, ETO~5		
45	383	315	235				Good,Tilted	1	H	235	Tilted UXO-Like, ETO~105	UXO-Like, ETO~150		
46	389	321	97			20"(+) ATV=321	Good,Tilted	1	H	97	UXO-Like, ETO~133, (POS=20")	UXO-Like, ETO~97	UXO-Like, ETO~87 (From TAR390, ATV168, Pos=-60")	ETO~10 (From TAR394, ATV 257, Latetime)
47	390	292	168			15"(-) ATV=292	Good,Tilted,Any Nearby Target?	1	H	292	Tilted UXO, ETO~90 (POS=-20")	Tilted UXO, ETO~163 (POS=20")	UXO-Like, ETO~103 (From TAR395 ATV 275, Pos=55")	
48	391	108	11			30"(+) ATV=108	Good,Tilted	1	H	11	Tilted UXO, ETO~108 (POS=30")	UXO-Like, ETO~100		
49	394	257	183			15"(+) ATV=257	Interfered	1	M	183	ETO~78, POS=-10",Small, shallow	UXO-Like, ETO~95, POS=-15"		
50	395	355	231	275		15"(+) ATV=355	Shallow, V. Plate	0	L	355	Non-UXO, ETO~-5, Shallow, Pos=15	Non-UXO, ETO~-20, Shallow, Pos=-20"		
51	396	350	229					0	L	350	ETO~82 Pos=-10"			
52	457	68	129	324	232		20" (-) ATV=120, good	0	L	68	Poor SCR	Poor SCR		
53	458	327	228			Shallow Plate	plate, with resonance in S11 on first pass and S22 on second pass	0	H	228	Non-UXO, ETO~60	Non-UXO, ETO~140		
54	459	210	276				10 inch offset, good	1	H	210	UXO-Like, ETO~30	UXO-Like, ETO~15		
55	460	5	248	126			25" (-) ATV=5	1	H	126	UXO-Like, ETO~0	EUXO-Like, ETO~40	UXO-Like,ETO~40	
56	462	160	227	83			plate?	0	L	227	Little or no Target Responses	Little or No Target response	Little or No Target response	
57	463	165	118	20				0	L	20	UXO-Like, ETO~165, POS=5"Small, Shallow	UXO-Like, ETO~30, POS=-20"	Non-UXO, ETO~120, POS=20"	
41	464	349	59					0	M	349	Non-UXO, ETO~170, Shallow, Small	Bad Scan		
59	470	158	61			V. UXO-Like	possible vert. Uxo	1	H	61	ETO~150	ETO~60		
60	471	140	27				s22 good, offset	1	H	140	UXO-Like or V. Plate, ETO~50	Severely Affected by 470		
61	472	320	200			Slightly tilted Plate		0	H	320	H. Plate, ETO~320	H. Plate, ETO~320		

No.	TAR.	Pass 1	Pass 2	Pass 3	Pass 4	General Comments	Proc. Note	GPR ID	Conf.	Best Pass ETO	Pass1 Feature Comments	Pass2 Feature Comments	Pass3 Feature Comments	
62	473	208	270	162		Empty ?	a -20 inch offset, surface clutter or plate?	0	L	270	Weak or NO Target Response	Weak or NO Target Response	Weak or No Target Response	
63	474	220	125	227		V. UXO-Like	15"(+) ATV=220	1	H	227	Tilted UXO-Like, ETO~35, POS=35"	Tilted UXO-Like, ETO~100, POS=40"	Tilted UXO, ETO~40, POS=35"	
47	475	178	83				18"(-) ATV=178	0	H	83	Non-UXO	Shallow Plate		
65	477	116	25	63		Deep V. UXO?		1	L	25	Weak or NO Target Response	UXO-Like, ETO~25, Deep, Poor SCR	Weak or No Target Response	
66	478	120	8	48		V. UXO-Like	Vertical UXO	1	H	48	V. UXO, ETO~120		V. UXO, ETO~48	
67	479	142	45			V. UXO-Like	Vertical UXO	1	H	45	V. UXO, ETO~142	V. UXO, ETO=45		
68	481	120	196			Shallow H. Plate	plate	0	H	120				
69	482	68	293	280	197	V. UXO		1	M	68	V. UXO, ETO~65	V. UXO, ETO~114		V. UXO, ETO~17
70	483	190	110	228			good s21	1	H	228	UXO-Like, ETO~150, POS=10"	Tilted UXO-Like, ETO~100	UXO-Like, ETO~145	
71	485	153	220			V. UXO-Like	good, Vertical UXO	1	H	220	ETO~153	ETO~40		
72	487	200	254	153			good	1	M	153	UXO-Like, ETO~16, (POS=-30")	UXO-Like, ETO~60	UXO-Like, ETO~64	
73	489	213	120			Varying ETO	good	0	M	213	UXO-Like, ETO~130	UXO-LIke, ETO~50, (POS=30")		
74	490	288	29				Good	1	H	29	UXO-Like, ETO~40	Tilted UXO, ETO~10		
75	494	5	64	301				0	L	301	Non-UXO, ETO=0	UXO-Like, ETO~0	Non-UXO, ETO~120	
76	497	100	337	226			Near Surface Plate	1	L	226	UXO-Like, ETO~16, Small, Shallow	Non-UXO, ETO~75, Weak	Tilted UXO-Like, ETO~57, Small	
77	500	185	79	288		Target Intended?	30"(-) ATV=185	0	L	185	UXO-Like, ETO~114, Small, Near Surface, POS=15"			
78	501	6	259				good	1	H	6	UXO-Like, ETO~108	UXO-LIke, ETO~76		
79	502	353	282	16			15"(+) ATV=353	0	L	282	UXO-Like, ETO~140, Pos=30"	Tilted UXO-Like, ETO~60, POS=--40"	Interfered responses	
80	504	345	255	196			10"(+) ATV=255	1	M	196	ETO~110, Poor SCR (Pos=-10")		UXO-Like, ETO~110 (POS=30"), Poor SCR	
81	508	180	223			Horizontal Bent Metal	good	0	M	180	UXO-Like, ETO~92, Pos=-5"	UXO-Like, ETO~144		
82	509	120	180			Horizontal Bent Metal	Good	0	H	120	UXO-Like, ETO~102, POS=0"	Tilted UXO-Like, ETO~180		
83	510	20	110	30		Poor SCR, Shallow or Deep		0	L	20	Non-UXO, ETO~16	Non-UXO, ETO~55	Tilted UXO-Like, ETO~25, POS=-25"	
84	513	256	304	0		Weak or None		0	L	256	Tilted UXO-Like, ETO~70, Weak,		UXO-Like, ETO~-4,	

No.	TAR.	Pass 1	Pass 2	Pass 3	Pass 4	General Comments	Proc. Note	GPR ID	Conf.	Best Pass ETO	Pass1 Feature Comments	Pass2 Feature Comments	Pass3 Feature Comments	
											Shaloow, Small		Weak, Shallow, Small	
85	520	185	96	300		Poor SCR,	10" (-) ATV1	0	L	185	Non-UXO, ETO~180, POS=0,Shallow, Small	ETO~88	Non-UXO, POS=10	
86	521	15	77	347		Offset		0	L	347	Weak or NO Target Response	Weak or NO Target Response	Weak or No Target Response	
87	523	9	101			0" & 30"(-) ATV=9	Shallow or Deep? Offset	0	L	9	Weak or NO Target Response		ETO=15	
88	526	9	120					1	H	120	UXO-Like, Offset to Side, ETO~100	Tilted UXO, ETO~119		
89	527	163	131			Offset		0	L	163	Non-UXO Plate, ETO~80	Non-UXO, Shallow		
90	531	158					Good	1	H	158	UXO-Like, ETO~160			
91	532	175	61	287				0	L	61	Weak or NO Target Response	UXO-Like, ETO~100, Weak	Weak or No Target Response	
92	535	297	23					1	L	297	UXO-Like, ETO~30, POS=30"	UXO-Like, ETO~23		
93	536	160	242	23		15"(+)ATV=160		1	H	160	UXO-Like, ETO~160	UXO-Like, ETO~160, Coupled with TAR 535	UXO-Like, ETO~126, POS=35"	
94	539	159	37			30"(+)ATV=159		1	H	37	Tilted UXO-Like, ETO~155, POS=30"	UXO-Like, ETO~132, POS=10		
95	540	158	50			High Clutter 10"(+)ATV=158	526	0	L	158	Weak or NO Target Response	Weak or NO Target Response		
96	543	332	225					0	H	225	Weak or NO Target Response	Weak or NO Target Response		
97	545	143	84	215		HF Filter 15"(-) ATV=215		1	L	215	Non-UXO, ETO~139, Shallow, Small, POS~--10"	UXO-Like, ETO~54, Shallow, Small, POS=-30"	UXO-Like, ETO~126, Shallow, Small, POS=--10"	

Bibliography

[1] C-C. Chen and L. Peters Jr., "Buried Unexploded Ordnance Identification via Complex Natural Resonances", *IEEE Transaction on Antennas and Propagation* , vol. AP-42, pp. 1645-1654, Nov. 1997.

[2] Jonathon D. Young, Leon Peters Jr. and C.-C. Chen, "Characteristic Resonance Identification Techniques for Buried Targets Seen by Ground Penetrating Radar", Chapter 5, "Detection and Identification of Visually Obscured Targets", Carl E. Baum, Published Taylor & Francis, 1998.

[3] C-C. Chen, M.B. Higgins, K. O'Neill and R. Detsch, “UWB Fully-polarimetric GPR Classification of Subsurface Unexploded Ordnance”, *IEEE Transactions on Geoscience and Remote Sensing*, Vol. 39, No.6, pp.1221-1230. M.B. Higgins,

[4] C.-C. Chen and K. O'Neill, “Improvement of UXO Classification Based on Fully-Polarimetric GPR Data,” *USA UXO/Countermine Forum*, New Oleans, April, 2001.

[5] Blossom Point Final ESTCP Report

[6] C-C. Chen, “A New Ground Penetrating Radar Antenna Design -- The Horn-Fed Bowtie (HFB)”, Antenna Measurement Techniques Association (AMTA) Symposium, October 1997.

[7] J.D. Young, K.A. Shubert and D.L. Moffatt, “Synthetic Radar Imagery,” *IEEE Transaction on Antennas and Propagation* , vol. AP-24, May 1976.

[8] S. Nag and L. Peters Jr., “Radar Images of Penetrable Targets Generated from Ramp Profile Functions,” *IEEE Transaction on Antennas and Propagation* , vol. AP-49, pp. 32-40, Jan. 2001.

[9] F. Shubitidze, K. O'Neill, K. Sun, and K.D. Paulsen, " Investigation of Broadband Electromagnetic Induction Scattering by Highly Conductive, Permeable, Arbitrarily Shaped 3-D Objects," submitted for publication, available on request.